CLASH: Weak-Lensing Shear-and-Magnification Analysis of 20 Galaxy Clusters

Cluster Lensing And Supernova survey with Hubble

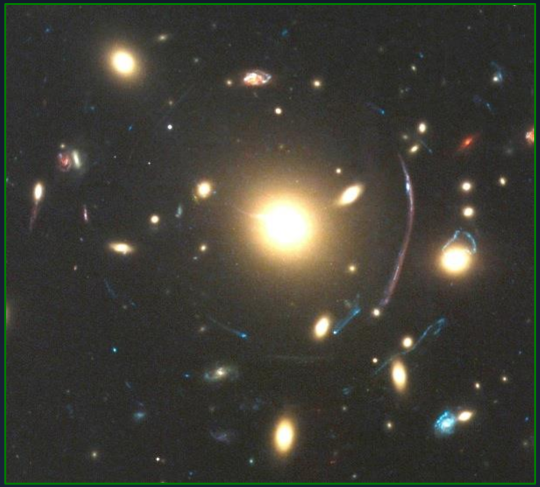

Keiichi Umetsu (ASIAA, Taiwan) with the CLASH team

Introduction

Clusters of Galaxies

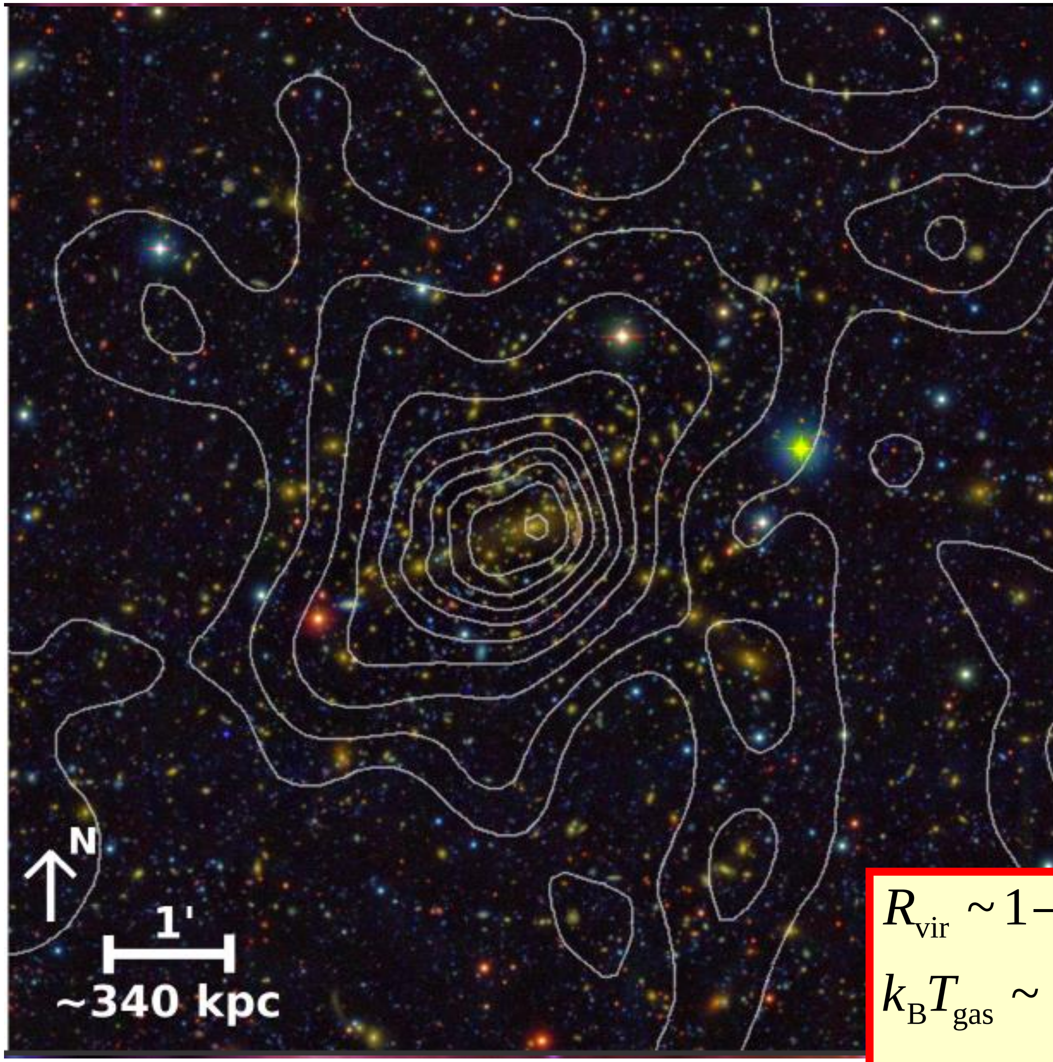

Clusters: the largest cosmic halos composed of 100-1000 galaxies.

tSZE by Bolocam

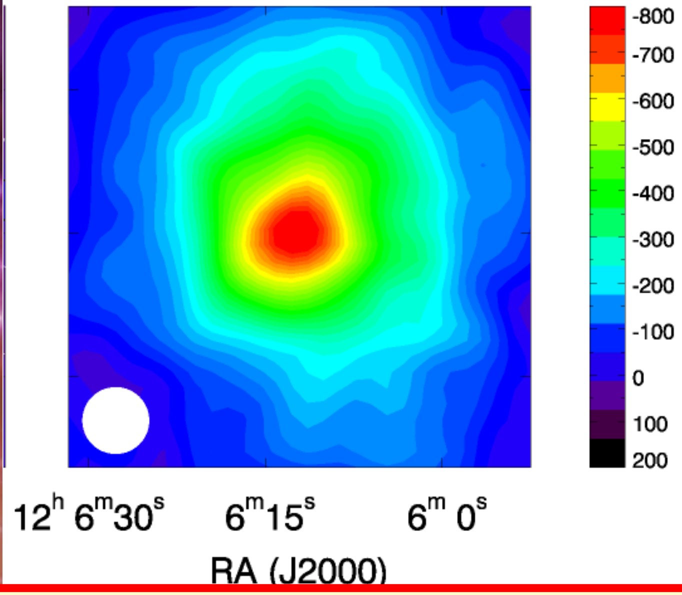

$$R_{\rm vir} \sim 1-2\,{\rm Mpc}$$

$$k_{\rm B} T_{\rm gas} \sim 3-10\,{\rm keV},\ \sigma_v = 800-1300\,{\rm km/s}$$

$$\Rightarrow M(R_{\rm vir}) \sim 2 R_{\rm vir} \sigma_v^2 / G \sim 10^{14-15} M_{\rm sun}$$

MACS1206 at z=0.44 (Umetsu+CLASH 12)

Clusters as the largest DM halos:

halos = gravitationally-bound nonlinear objects

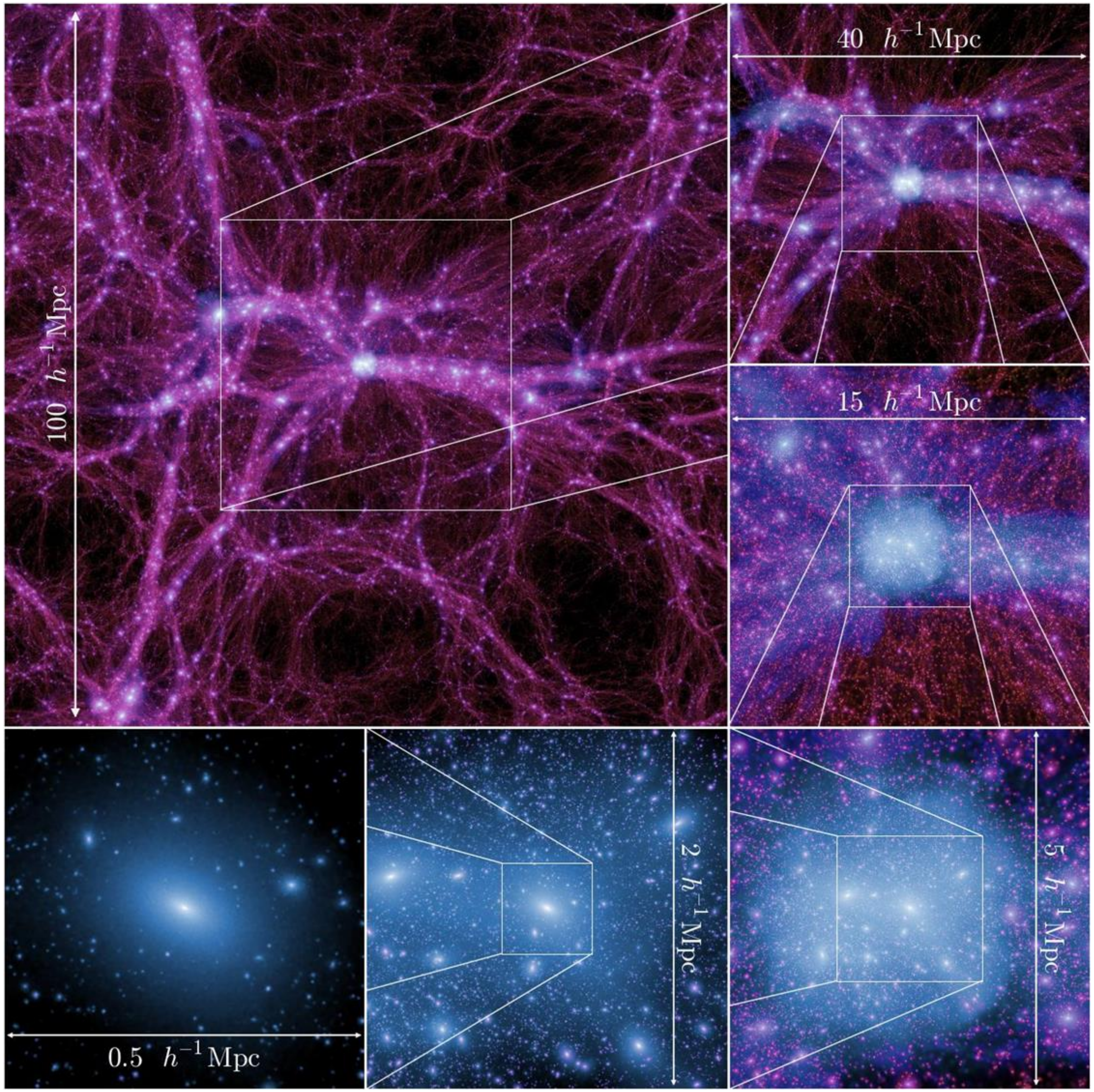

Clusters are formed at the intersection of filaments and sheets (LSS).

Inner halos are more triaxial (collisionless nature of DM)

Abundant substructures (CDM)

Boylan-Kolchin+09

Clusters as Cosmological Probe

Cluster # counts $$\frac{dN(>M_{\lim},z)}{d\Omega dz} = \int_{M_{\lim}}^{\infty} dM \boxed{\frac{dV(z)}{d\Omega dz}} \boxed{\frac{d^2 n}{dVdM}(M,z)}$$

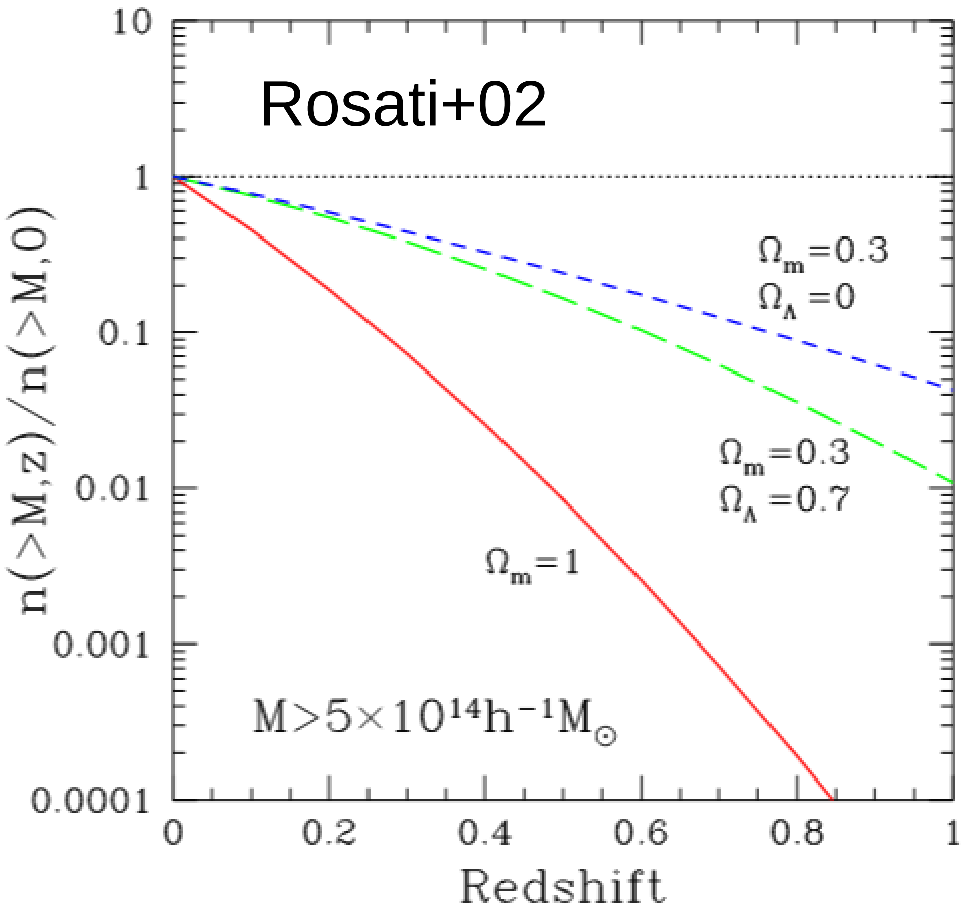

Volume element

$$\frac{d^2V}{dzd\Omega} = \frac{cr^2[\chi(z)]}{H(z)}, \quad \chi(z) = \int_0^z \frac{dz'}{H(z')}$$

Halo mass function

$$\frac{d^2n}{dVdM}(M,z) \propto \exp\left[-\frac{\nu^2}{2}\right]$$

$$\nu \equiv \frac{\delta_c}{D_+(z)\sigma(M)} \sim 3 \text{ for clusters}$$

Cluster counts are exponentially sensitive to *cosmology* and ***cluster mass calibration***!

Key Predictions of nonlinear structure formation models

(1) Quasi self-similar DM-halo density profiles

Quasi-universal Halo Density Profile for collisionless CDM

Spherically-averaged DM density profiles <ρ(r)> from numerical simulations

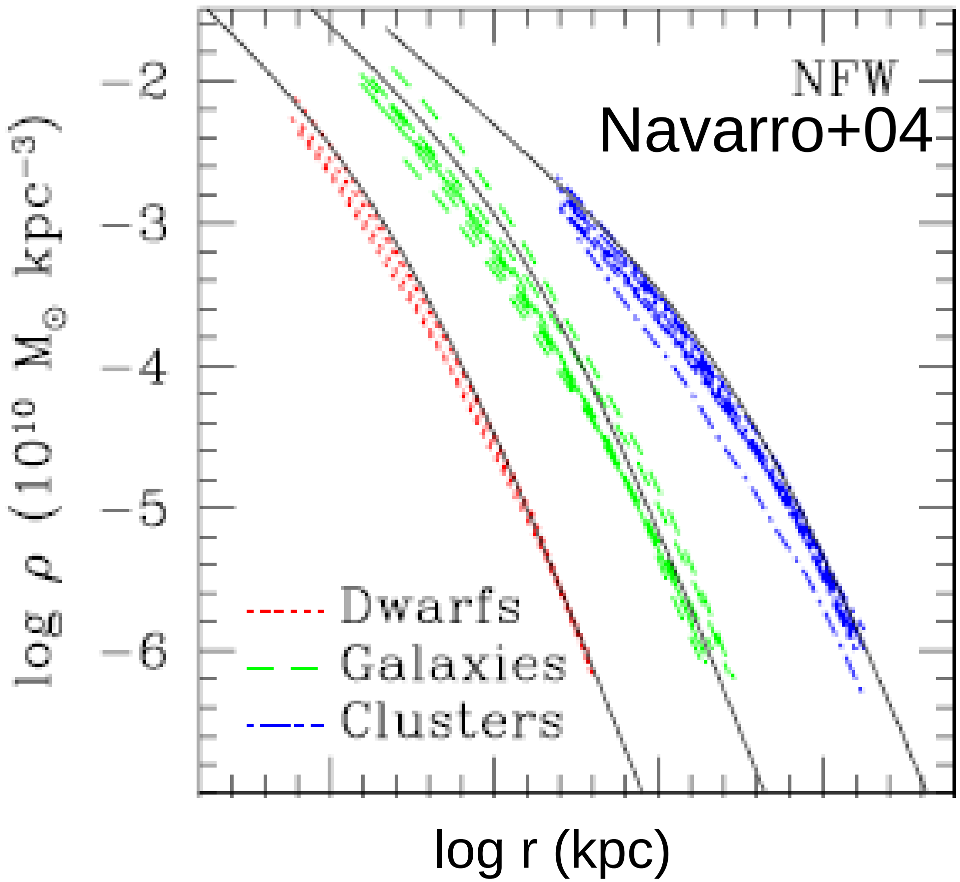

Self-similarity

$$\rho(r) = Af(r/r_s)$$

Empirical fitting formula by Navarro-Frenk-White (NFW)

$$\rho(r) = \frac{\rho_s}{(r/r_s)(1+r/r_s)^2}$$

Nearly independent of halo mass, redshift, initial conditions, and cosmology (NFW96, 97)

“Diversity” of halo density profiles

Mass profiles of DM halos are not strictly self-similar:

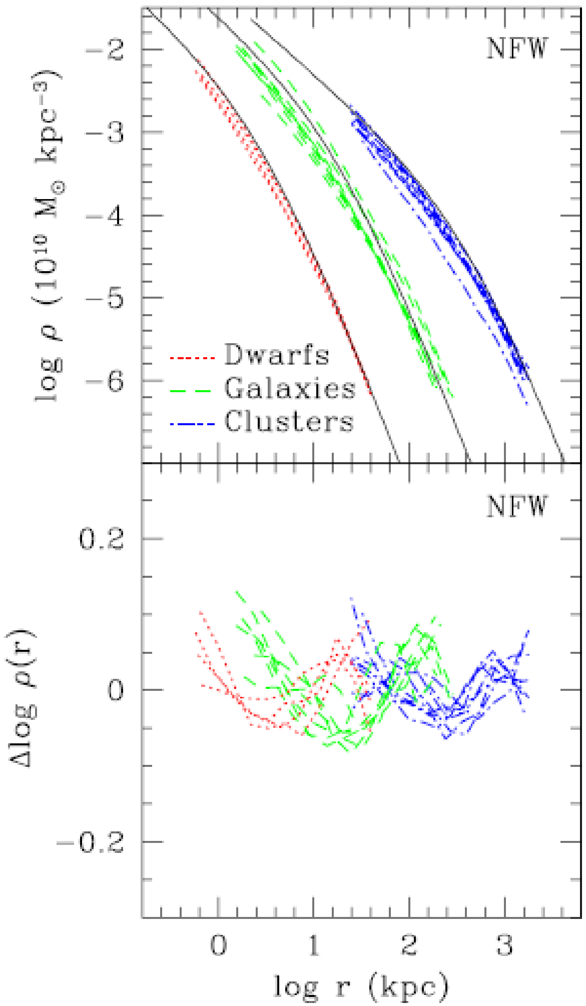

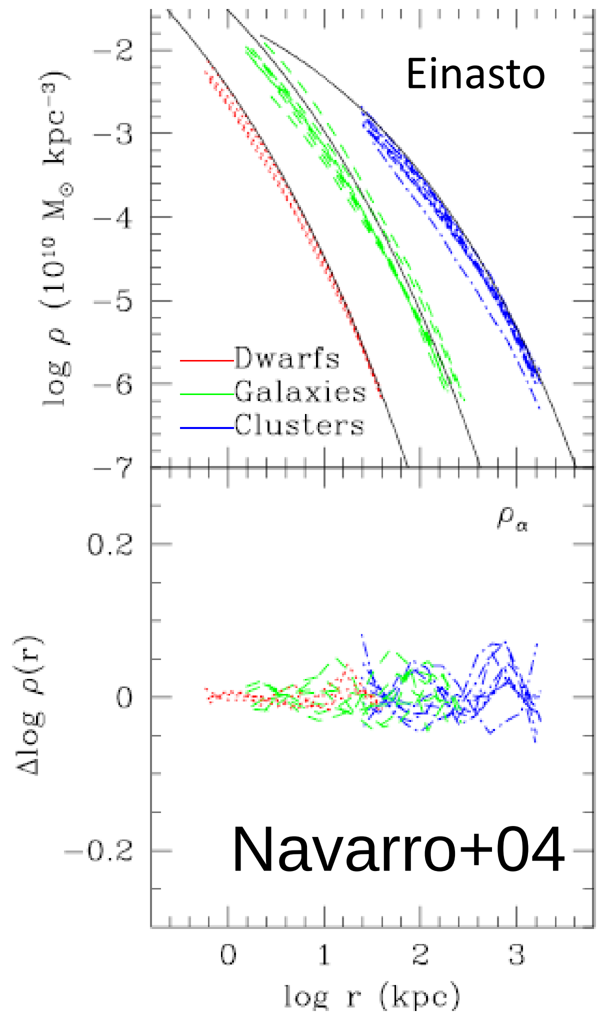

Einasto profile (ρ_s, r_s, α)

$$\frac{d \ln \rho(r)}{d \ln r} = -2\left(\frac{r}{r_s}\right)^{\alpha}$$

α: degree of curvature

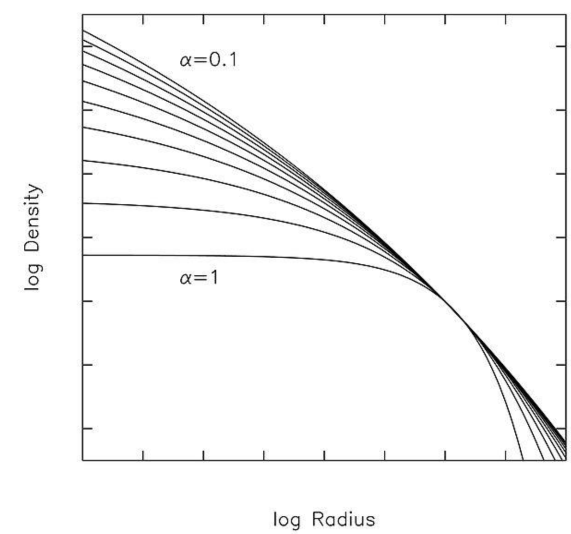

Key Predictions of nonlinear structure formation models

(2) Halo concentration-mass (c-M) relation

Degree of mass concentration

$$c_{200}(M_{200}) \equiv \frac{r_{200}}{r_s} \Rightarrow \frac{\text{Virial radius}}{\text{Isothermal (scale) radius}}$$

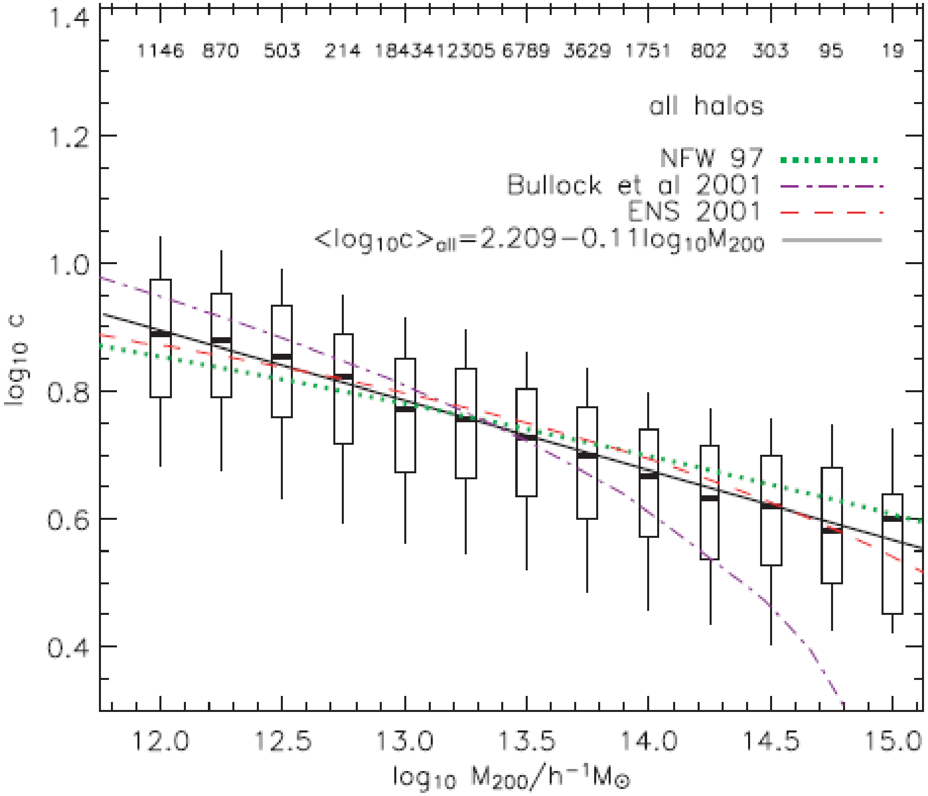

In hierarchical structure formation, <*c*> is predicted to decrease with increasing *M*

DM halos that are more massive collapse later on average, when the mean background density ρ_b of the universe is correspondingly lower (Bullock+01; Neto+07)

Clusters in a concordance LCDM cosmology are predicted to have $\langle c_{200} \rangle$=3-4 (Gao+08; Duffy+08; Bhattacharya+13)

Intrinsic Scatter in c(M): Mass Assembly Histories (MAH)

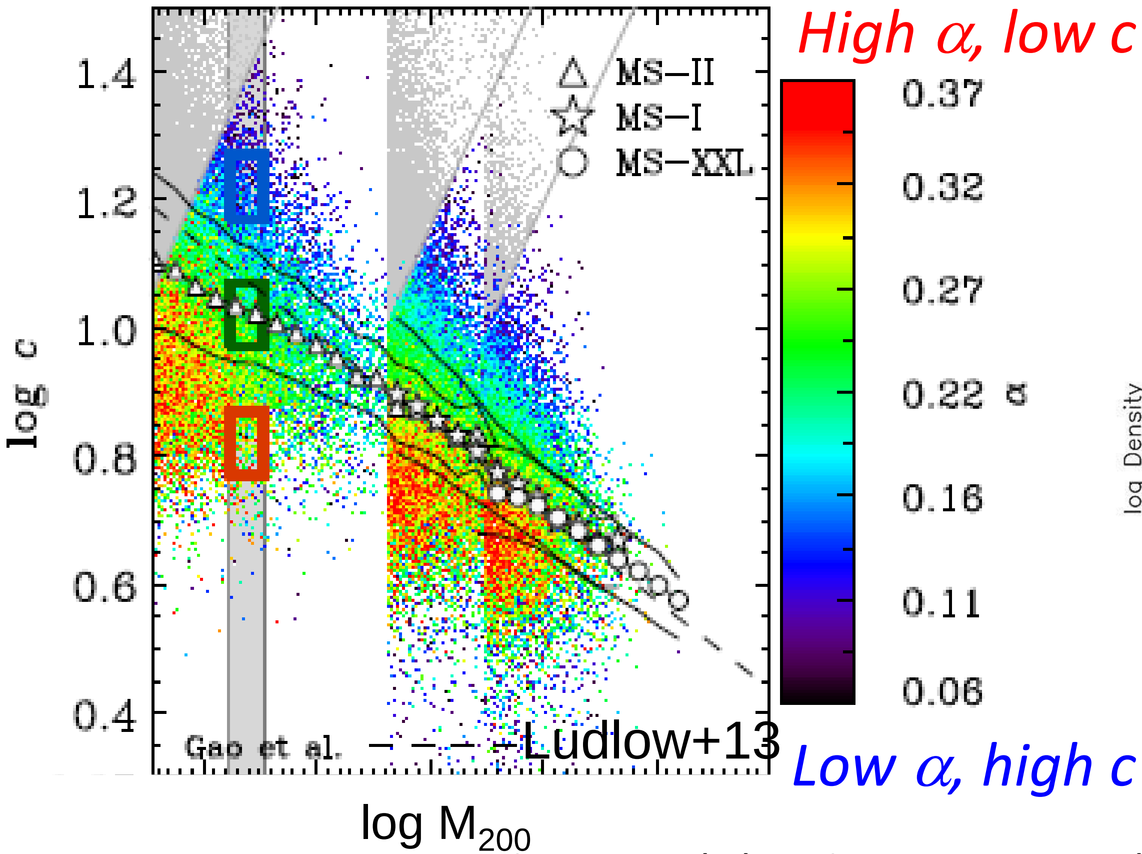

α: degree of curvature

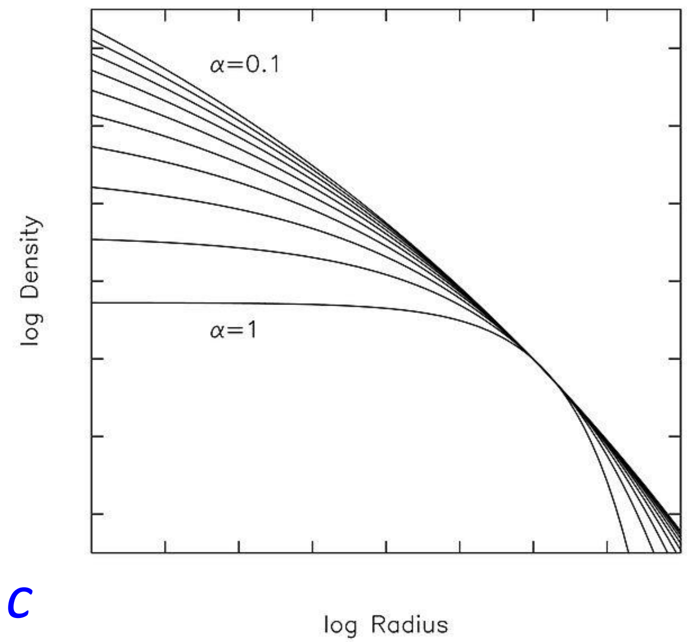

- Scatter is due to another DoF (α), related to MAH (Ludlow+13)
- Larger or smaller values of α correspond to halos that have been assembled more or less rapidly than the NFW curve
- Clusters with average c_{200} have the NFW-equivalent α ~0.18

Key Predictions of nonlinear structure formation models

(3) Halo bias: surrounding large-scale structure

Halo bias: $b_h(M,z)$

2h term

Clustering of matter around halos with M:

$$\xi_{hm}(r\,|\,M) = \frac{\langle \rho_{1h}(r\,|\,M)\rangle}{\bar{\rho}} + \boxed{b_h(M)\xi_{mm}(r)}$$

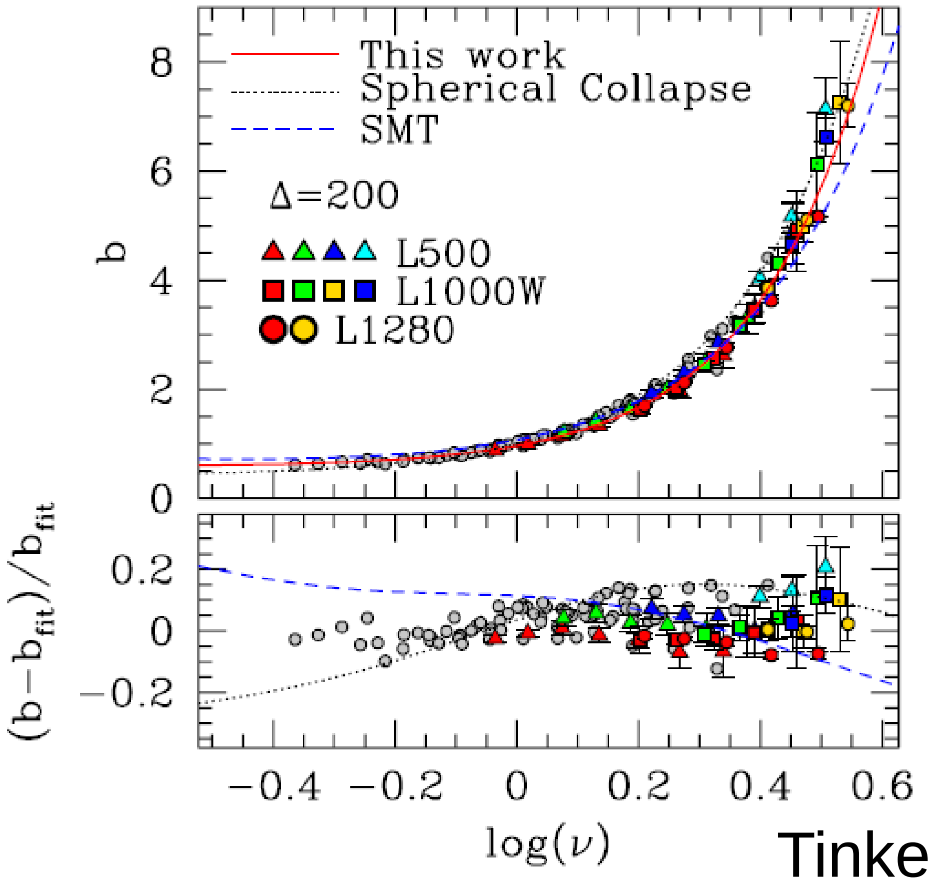

$$b_h(\nu) \approx 1 + \frac{\nu^2 - 1}{\delta_c}$$

$$\nu \equiv \frac{\delta_c}{\sigma(M,z)} \sim 3-4 \text{ for clusters}$$

$(\log_{10}\nu \sim 0.5\text{-}0.6)$

<u>Typical cluster formation epoch:</u>

z_f = 0.7 – 0.5 (Boylan-Kolchin 08)

Tinker+10 LCDM simulations

Weak Gravitational Lensing

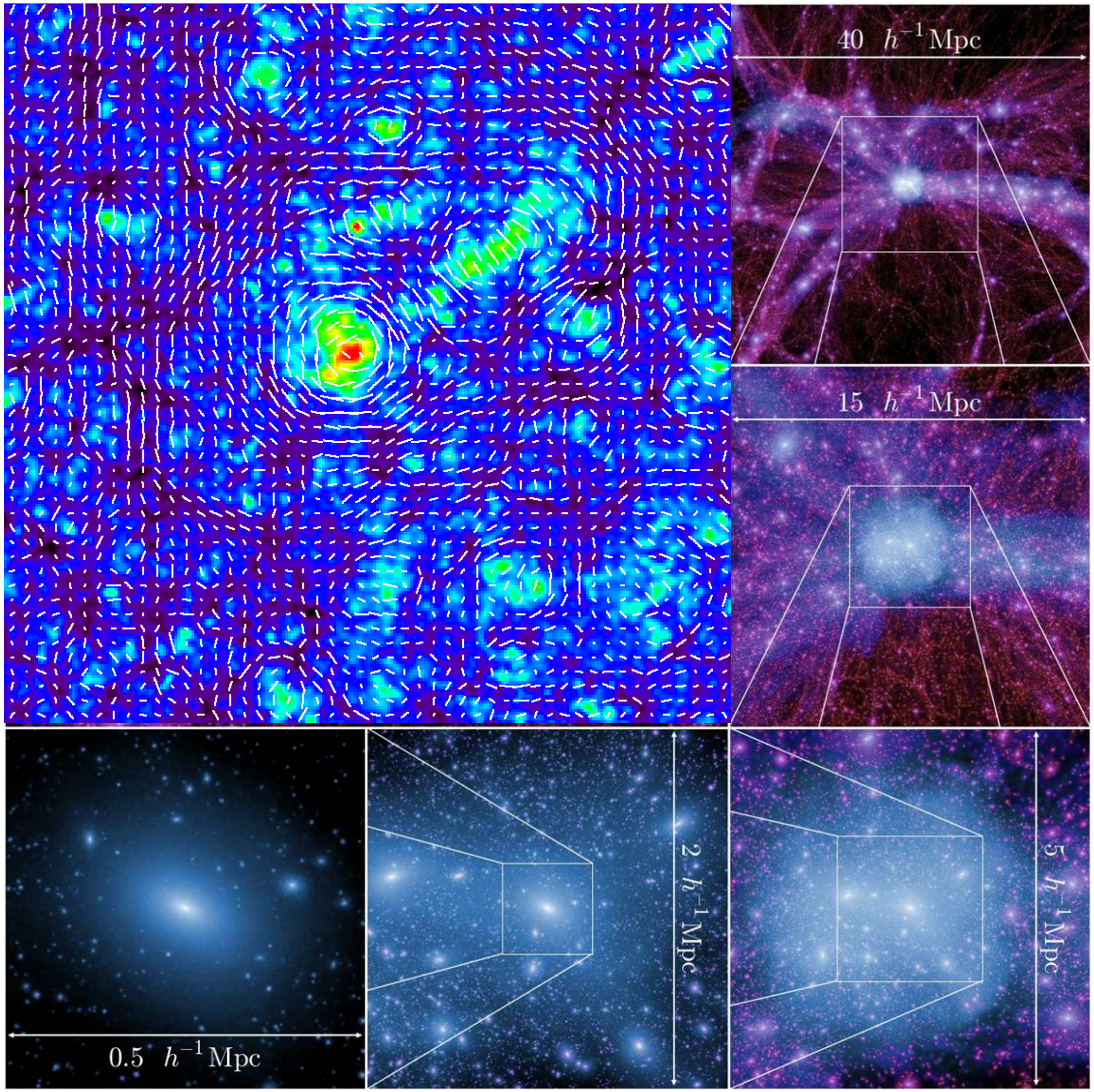

Objectives

Halo structure (1h)

- ✓ *Virial mass, M_{200}*:
- ✓ Halo density profile, $\langle\rho(r)\rangle$:
- ✓ *Concentration, $c(M,z)$*:

Surrounding LSS (2h)

- ✓ Halo bias $b(M,z)$
- ✓ Primordial matter $P(k)$

Gravitational Shear

$$\gamma = \partial\partial\Phi / 2$$

$$\partial := \partial_x + i\partial_y = e^{i\phi}\partial_r$$

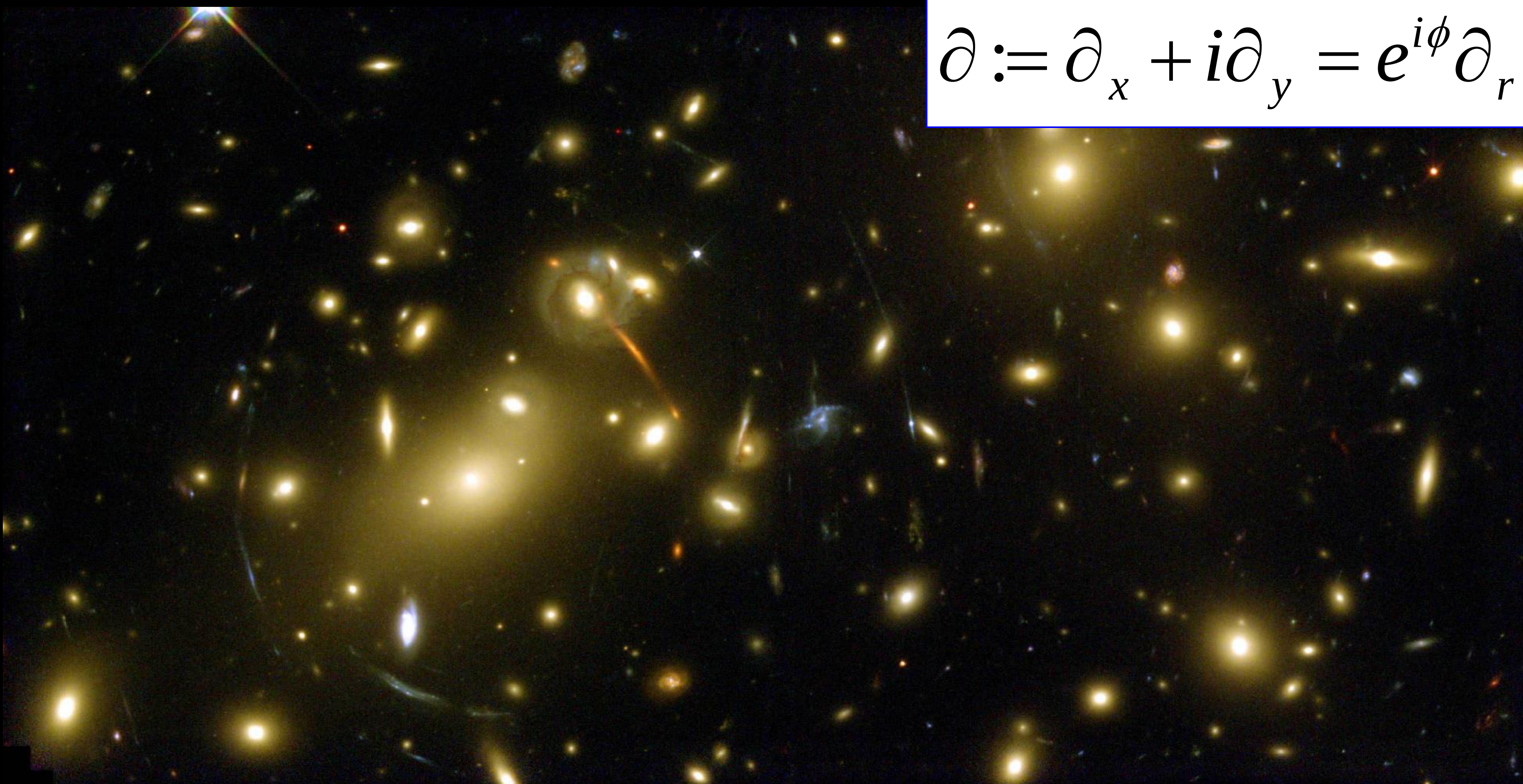

Tangential Shear

Measure of azimuthally-averaged tangential coherence of elliptical distortions around a given point (Kaiser 95):

$$\gamma_+(R) = \Delta\Sigma(\mathrm{R}) / \Sigma_{\mathrm{crit}}$$

$$\gamma_\times(R) = 0$$

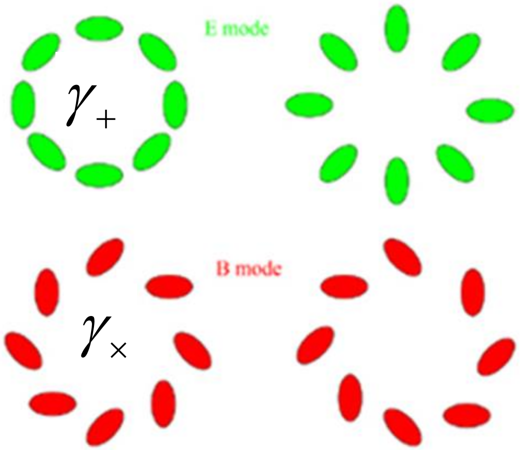

ΔΣ(R) is the radially-*modulated* surface mass density:

$$\Delta\Sigma(R) = \Sigma(< R) - \Sigma(R)$$

Sensitive to interior mass

$$\Sigma = \int dl \delta\rho$$

$\Sigma_{crit}(z_l,z_s)$ is the *critical surface mass density of lensing*

Shear doesn't see mass sheet

Averaged lensing profiles in/around LCDM halos (Oguri+Hamana 11)

Total

$$\kappa = \Sigma(R) / \Sigma_{\rm crit}$$

Modulated

$$\gamma_+ = \Delta\Sigma(R) / \Sigma_{\rm crit}$$

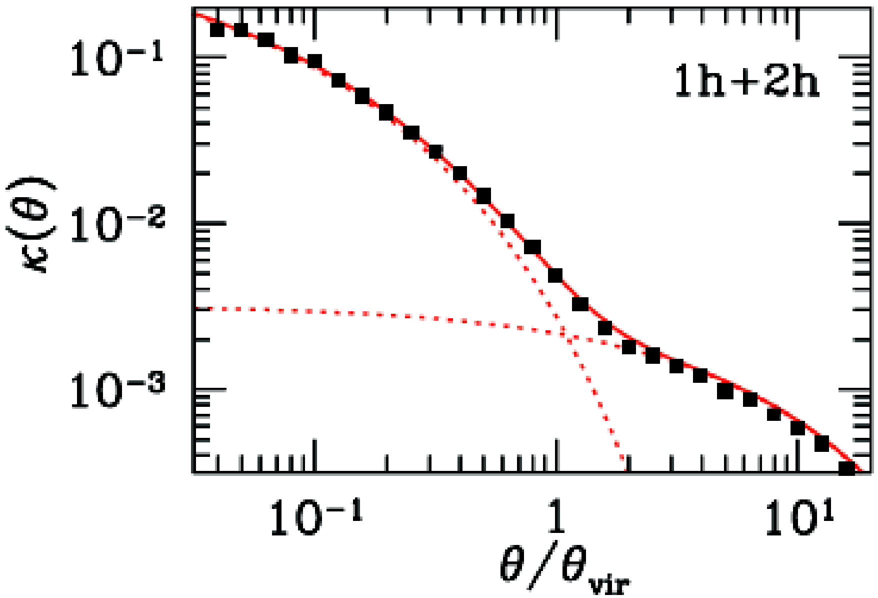

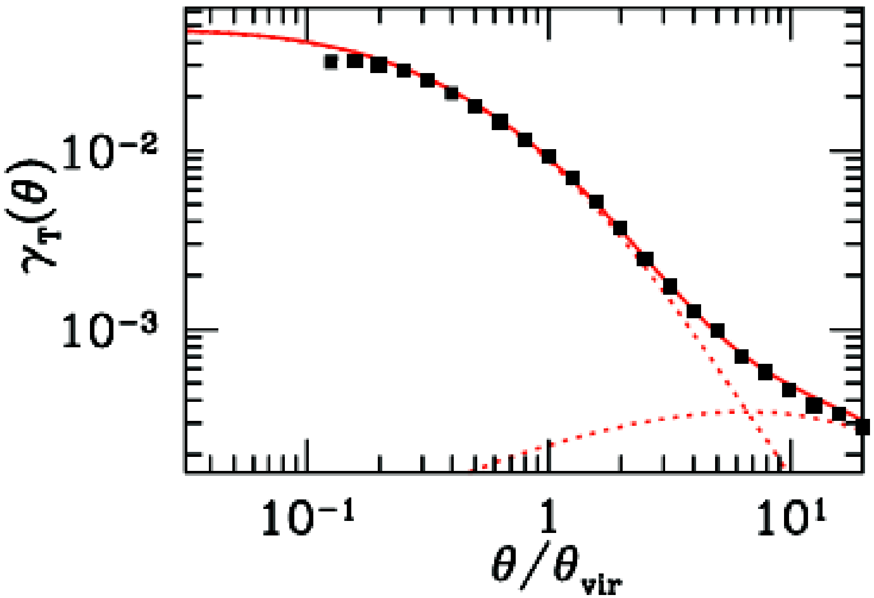

- **Tangential shear is a powerful probe of 1-halo term, or internal halo structure.**
- **Shear alone cannot recover absolute mass, known as *mass-sheet degeneracy***

Non-local substructure effect

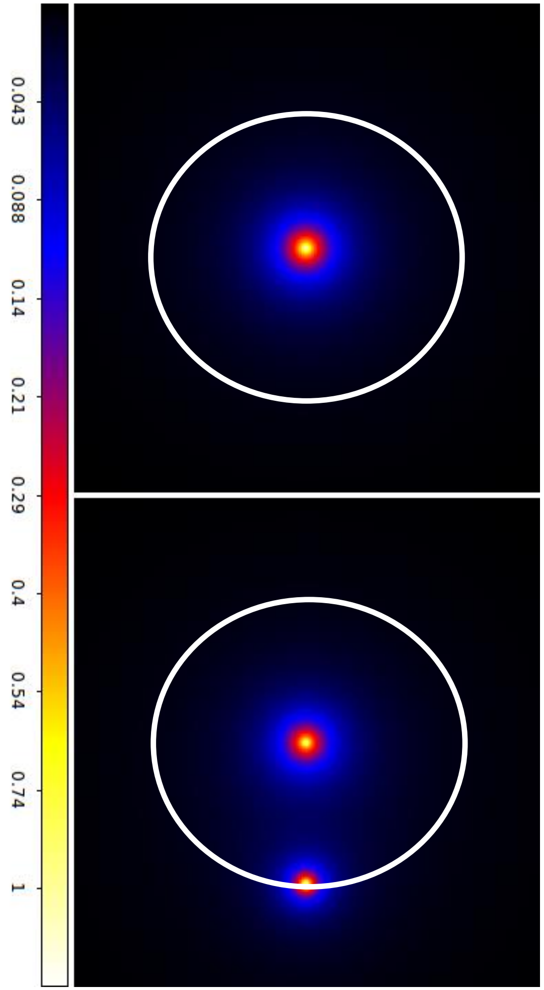

A substructure at R ~ r_{vir} of the main halo, modulating $\Delta\Sigma(R) = \Sigma(<R) - \Sigma(R)$

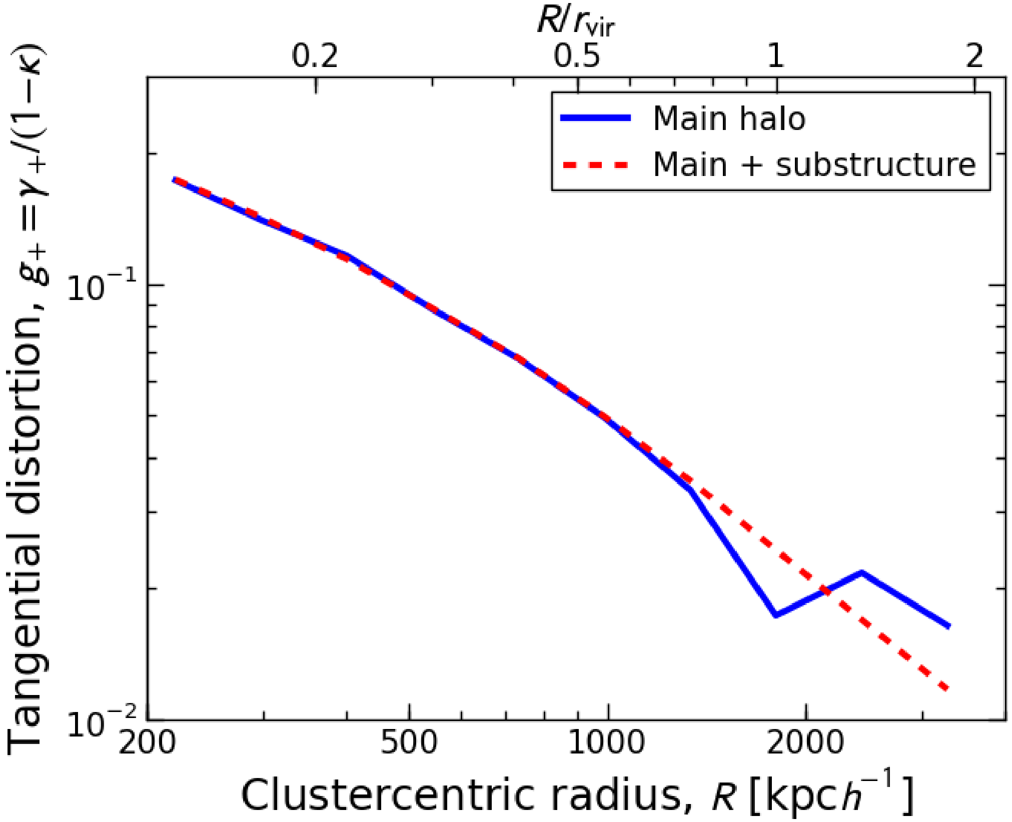

Known ~10% negative bias in mass estimates from tangential-shear fitting, inherent to clusters sitting in substructured field (Rasia+12)

Gravitational Magnification

$$\kappa = \partial\partial^{*}\Phi / 2 = \Delta\Phi / 2$$

$$\partial := \partial_x + i\partial_y = e^{i\phi}\partial_r$$

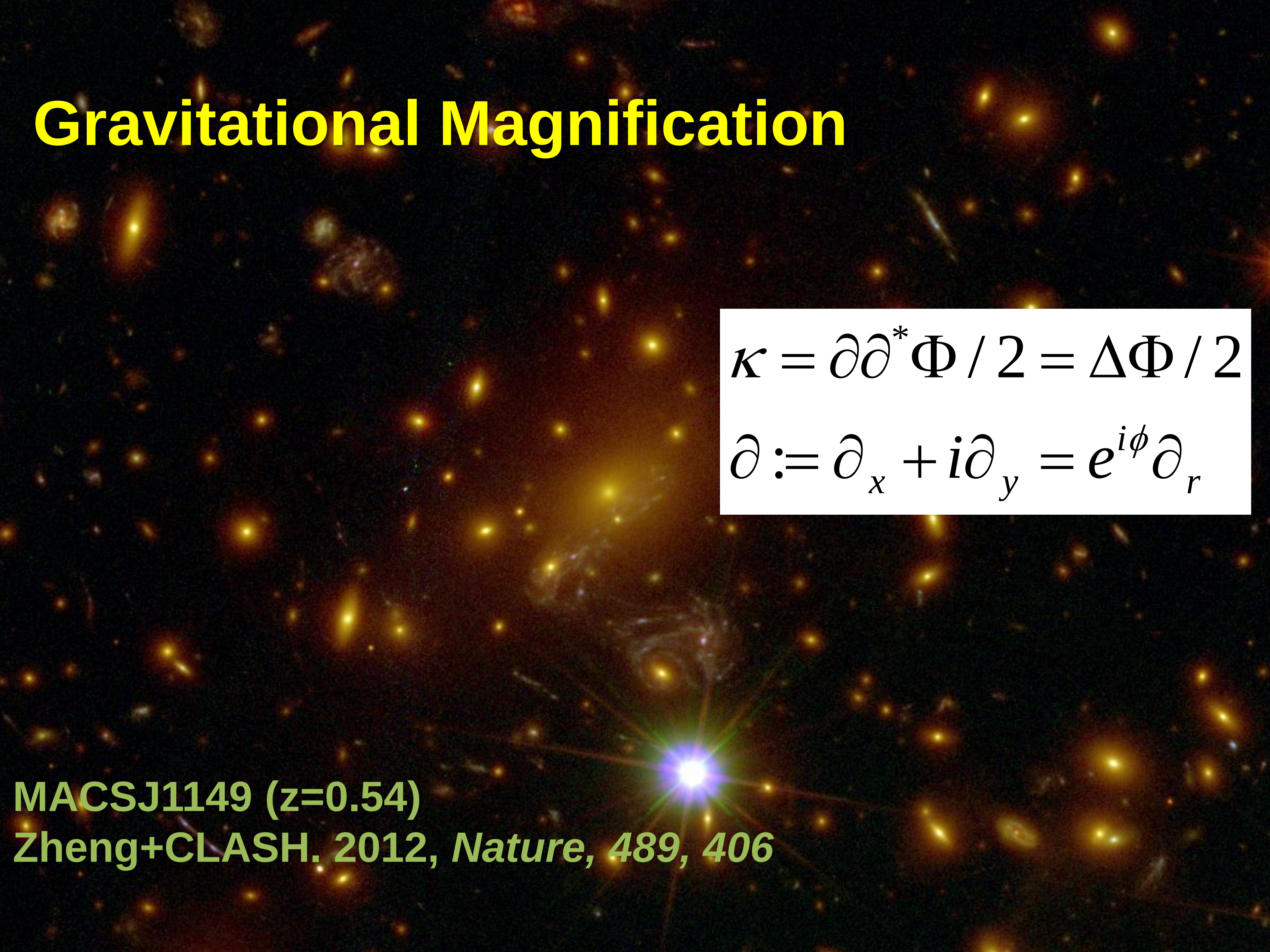

MACSJ1149 (z=0.54)
Zheng+CLASH. 2012, *Nature, 489, 406*

Magnification Effects

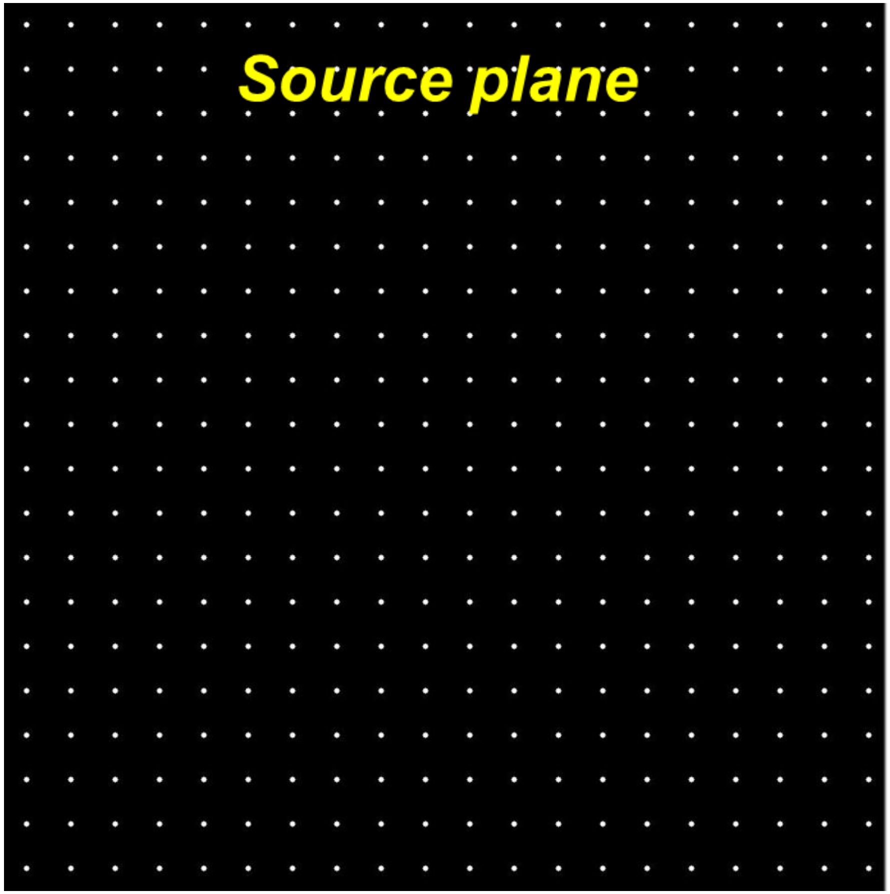

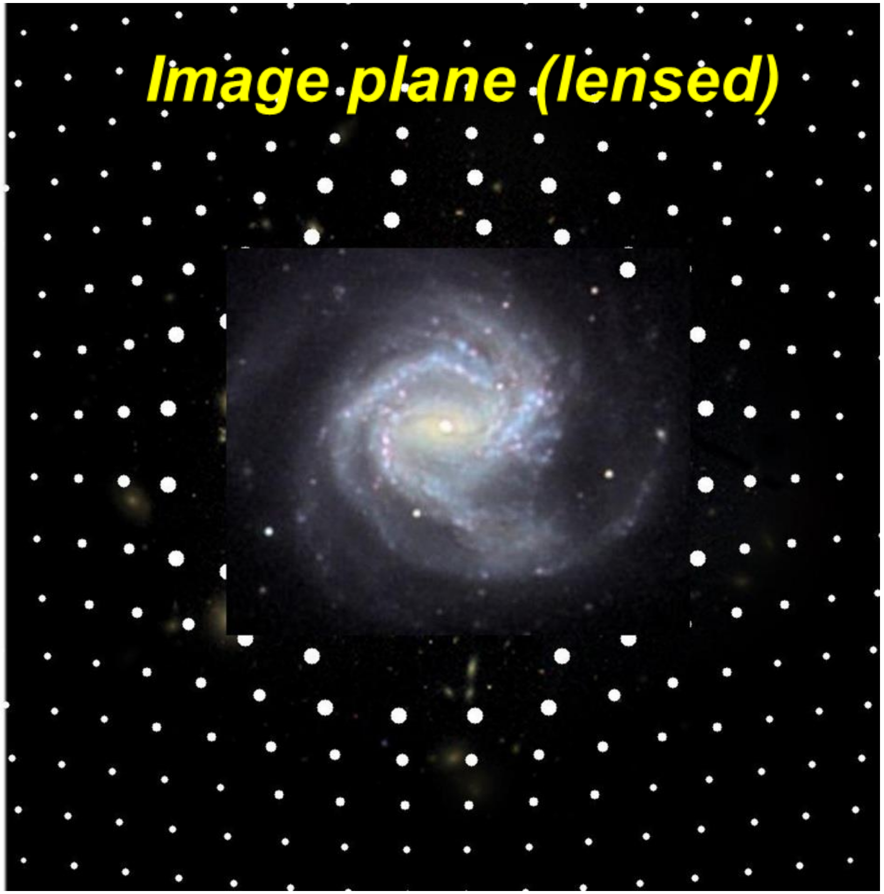

- Image flux, *F*: $\mu \sim 1+2\kappa$
- Image size, *r*: $\mu^{1/2} \sim 1+\kappa$
- $\boxed{\text{Sky area, } \Delta\Omega\text{: } \mu \sim 1+2\kappa}$

Sensitive to "local" matter density

$$\kappa = \Sigma / \Sigma_{\rm crit}$$

Negative Magnification Bias: Count Depletion

Geometric shear-magnification consistency

Number counts of red galaxies at <z>~1 highly depleted

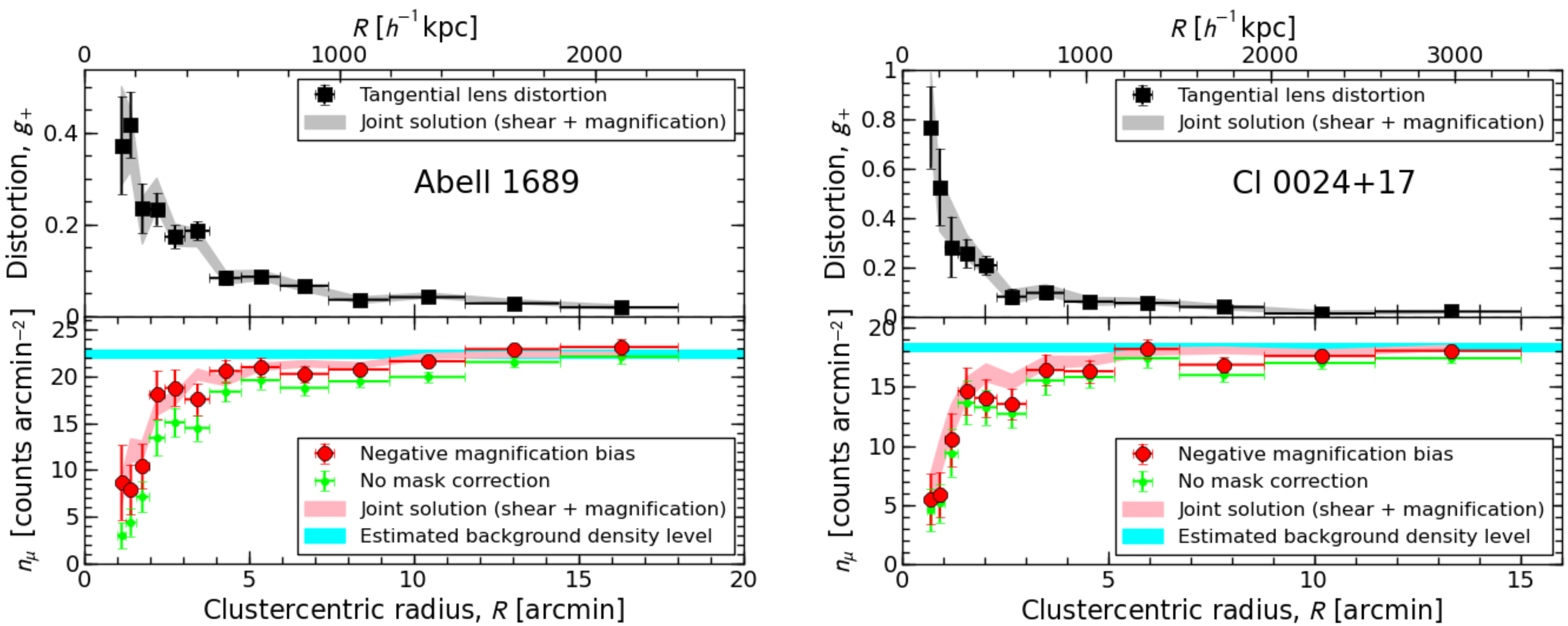

Umetsu+11a, ApJ, 729, 127

Subaru telescope data

Combining Shear and Magnification

Bayesian joint-likelihood analysis (Umetsu+11a; Umetsu 13)

Shear + magnification

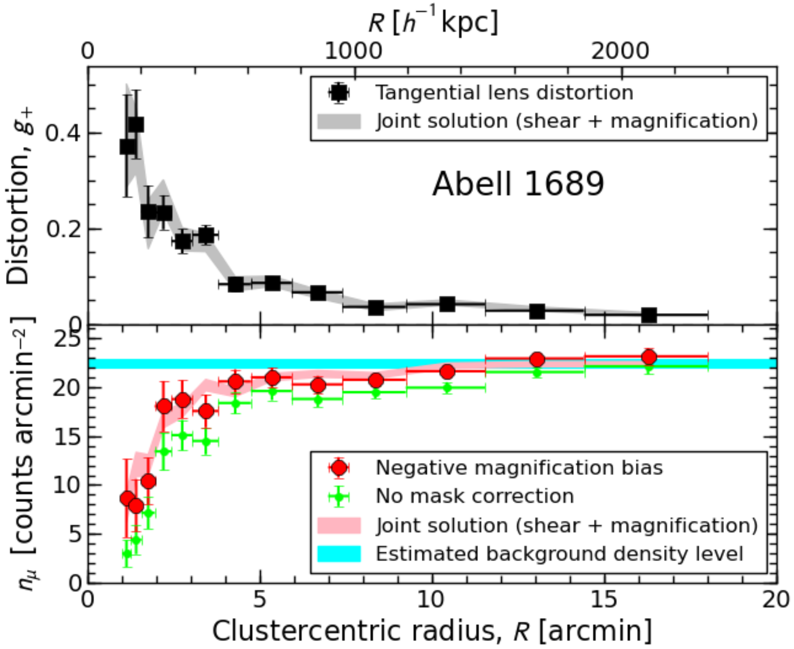

Non-parametric Σ(R) solution

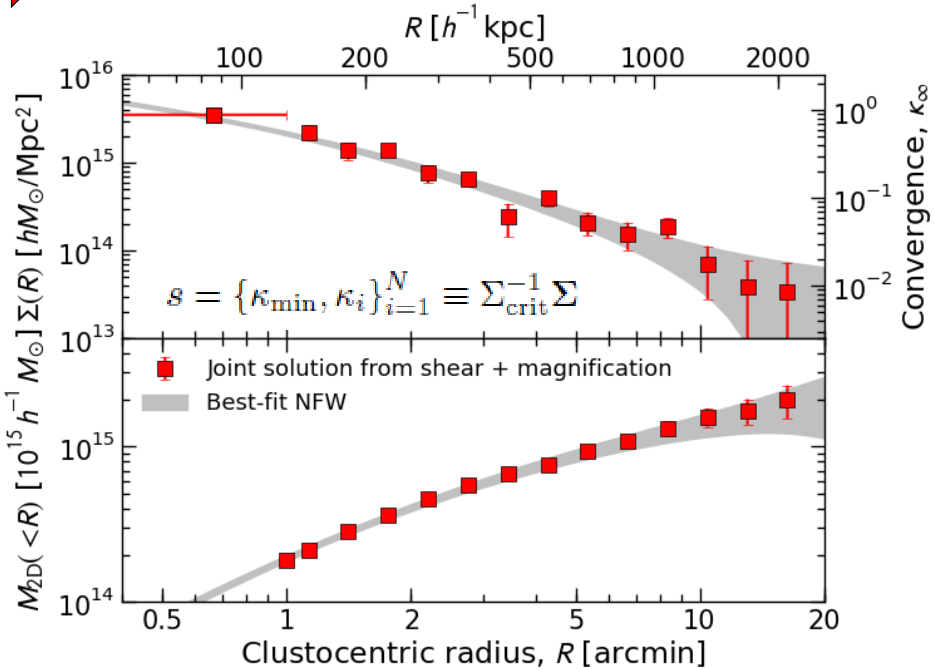

- Mass-sheet degeneracy broken
- Total statistical precision improved by ~20-30%
- Calibration uncertainties marginalized over: $c = \{\langle W \rangle_s, f_{W,s}, \langle W \rangle_\mu, \overline{n}_\mu, s_{\rm eff}\}$.

CLASH:

Cluster Lensing And Supernova survey with Hubble

A 524-orbit HST Multi-Cycle Treasury Program designed to place new constraints on the fundamental components of the cosmos: dark matter, dark energy, and baryons (PI: Marc Postman, STScI)

Wide-field Subaru imaging (0.4 - 0.9 μm) plays a unique role in complementing deep HST imaging of cluster cores.

My talk will focus on CLASH-WL results based primarily on Subaru data (Umetsu+CLASH 14, arXiv:1404.1375)

SUBARU multi-color maging for wide-field weak lensing

High-resolution space imaging with *Hubble* for strong lensing

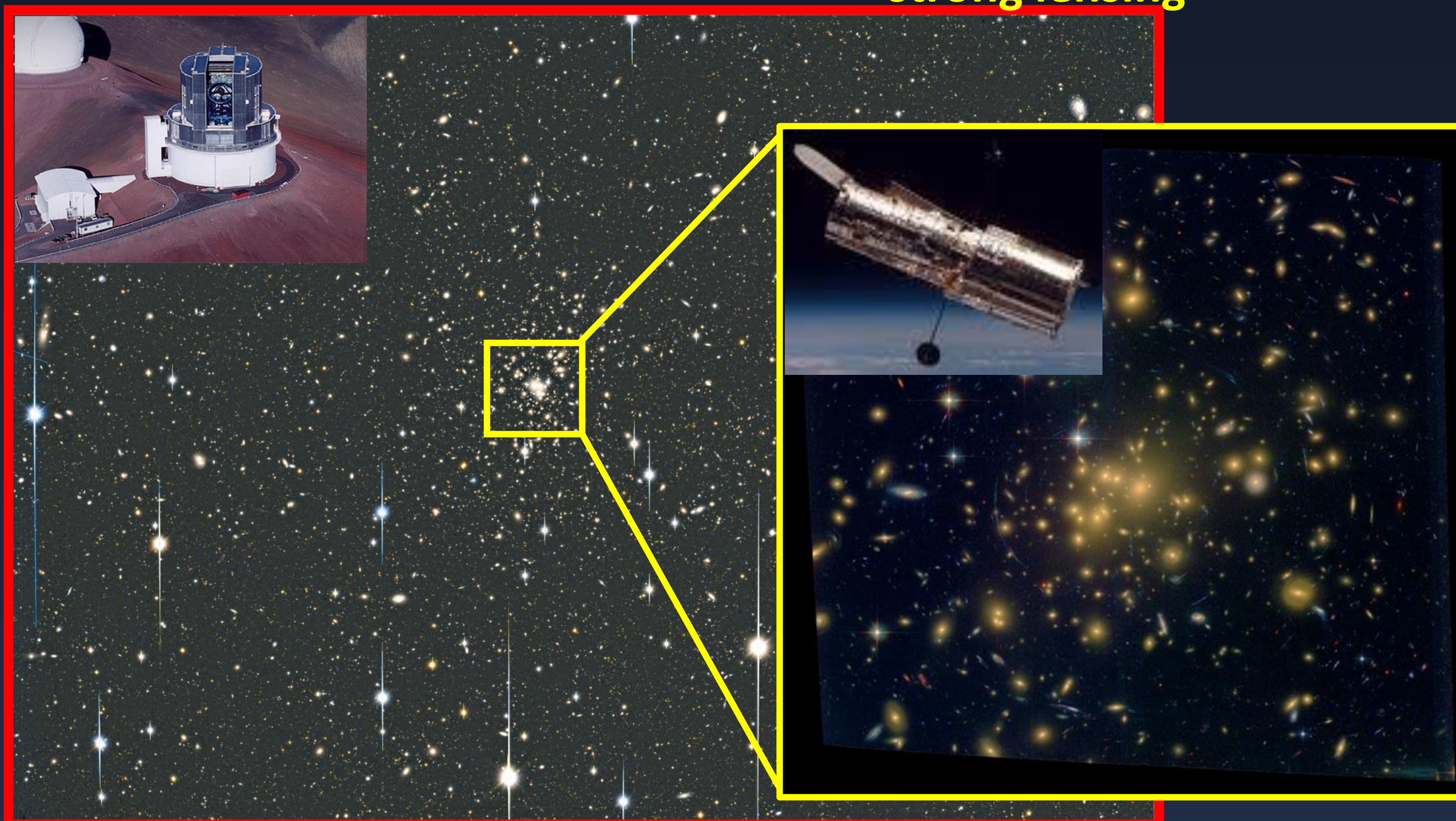

SUBARU shear strength as a function of magnitude

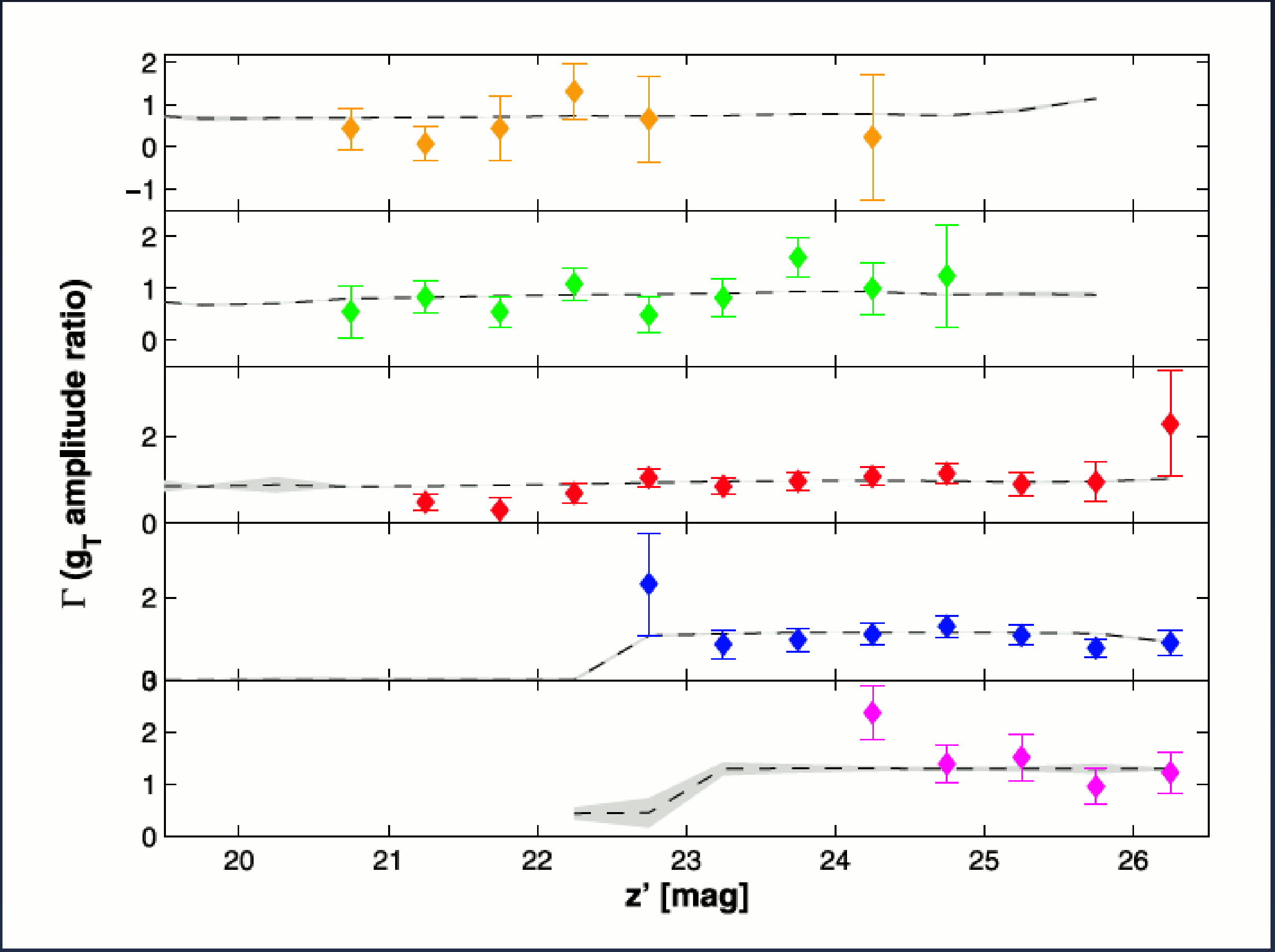

Medezinski, Broadhurst, Umetsu+11

Pre-CLASH Lensing Results

Strong-lensing (*HST*) + shear + magnification (Subaru) available only for a handful of **strong-lensing-selected** high-mass clusters (θ_E > 30 arcsec, zs=2)

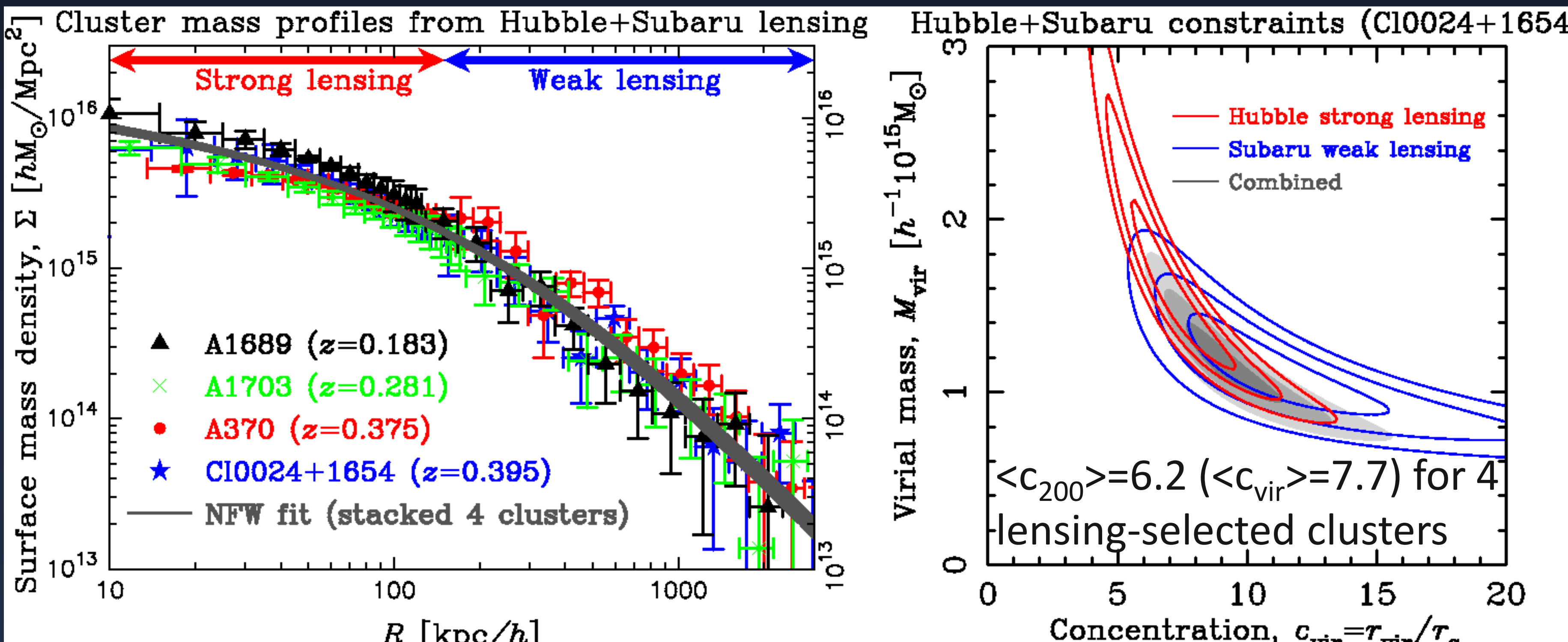

<c_{200}>=6.2 (<c_{vir}>=7.7) for 4 lensing-selected clusters

Umetsu+2011a, Umetsu et al. 2010

Pre-CLASH Lensing Results

Strong-lensing (*HST*) + shear + magnification (Subaru) available only for a handful of **strong-lensing-selected** high-mass clusters (θ_E > 30 arcsec, zs=2)

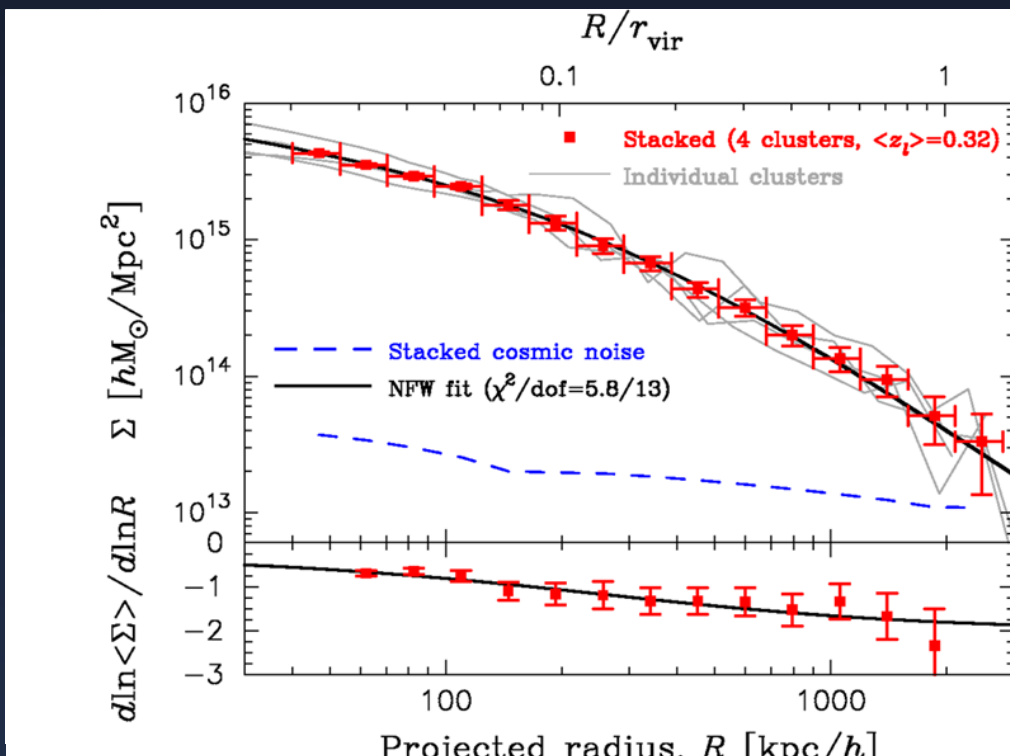

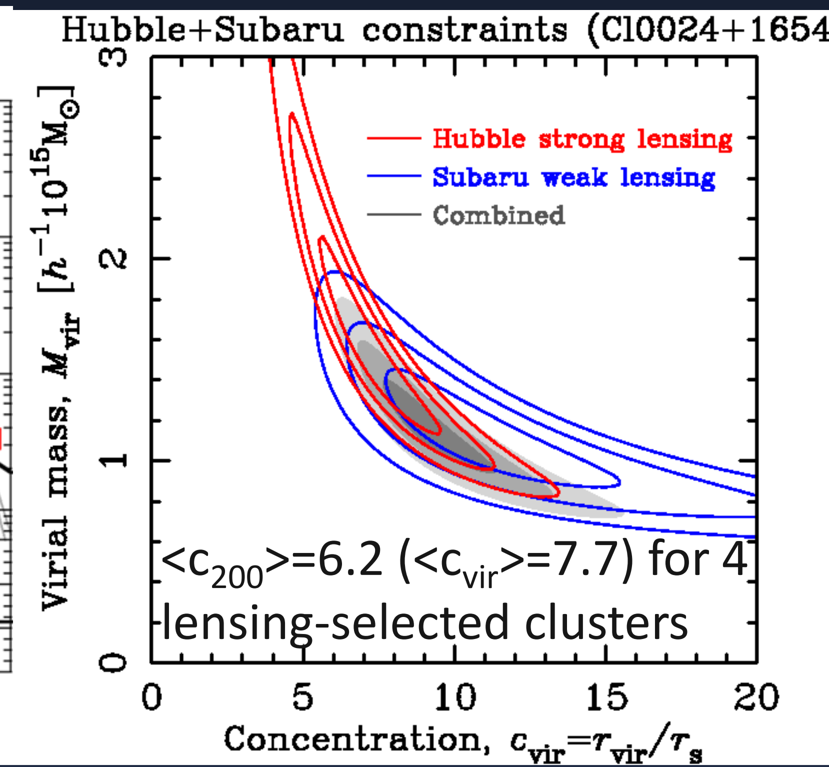

Umetsu+2011b, Umetsu et al. 2010

Pre-CLASH Lensing Summary

1. Cluster mass profile "shape"
   – NFW is an excellent fit out to ~Rvir (cf. Okabe, Smith, Umetsu+13; Newman+13)
   – Consistent with collisionless, non-relativistic DM
2. Degree of halo concentration
   – c_{200} ~ 6 at M_{200} = 1.2e15Msun/h (z=0.32) assuming spherical NFW
   – Higher than LCDM predictions, $\langle c_{200} \rangle$~3 for high-mass clusters
   – Expected lensing-selection/projection bias ~ +50%: $\langle c_{200} \rangle$~4.5 *not enough??*

CLASH Targets & Objectives

1. 20 X-ray hot/regular clusters
   – Individual and ensemble-averaged DM density profiles $\langle\rho(r)\rangle$ in equilibrium clusters
   – Cluster c-M relation, c(M)
2. 5 high-magnification clusters
   – Search for high-z magnified galaxies

Postman+CLASH 2012, ApJS

The CLASH Gallery (HST)

The final HST observation for CLASH was on 9-July-2013 … 963 days, 15 hrs, 31 min after first obs.

CLASH X-ray-selected subsample

- Redshift coverage
  - $0.18 < z < 0.90$
- No lensing selection bias
- X-ray hot (T_x>5keV)
  - M_{200} = [5-20] 1e14M_{sun}/h
- Small BCG to X-ray-peak offset
  - Offset dispersion: $\sigma_{off} \sim$ 10kpc/h
- Smooth, regular X-ray morphology

→ Optimized for radial profile measurements

Allen et al. 2004; Schmidt & Allen 2007; Allen et al. 2008; Mantz et al. 2010

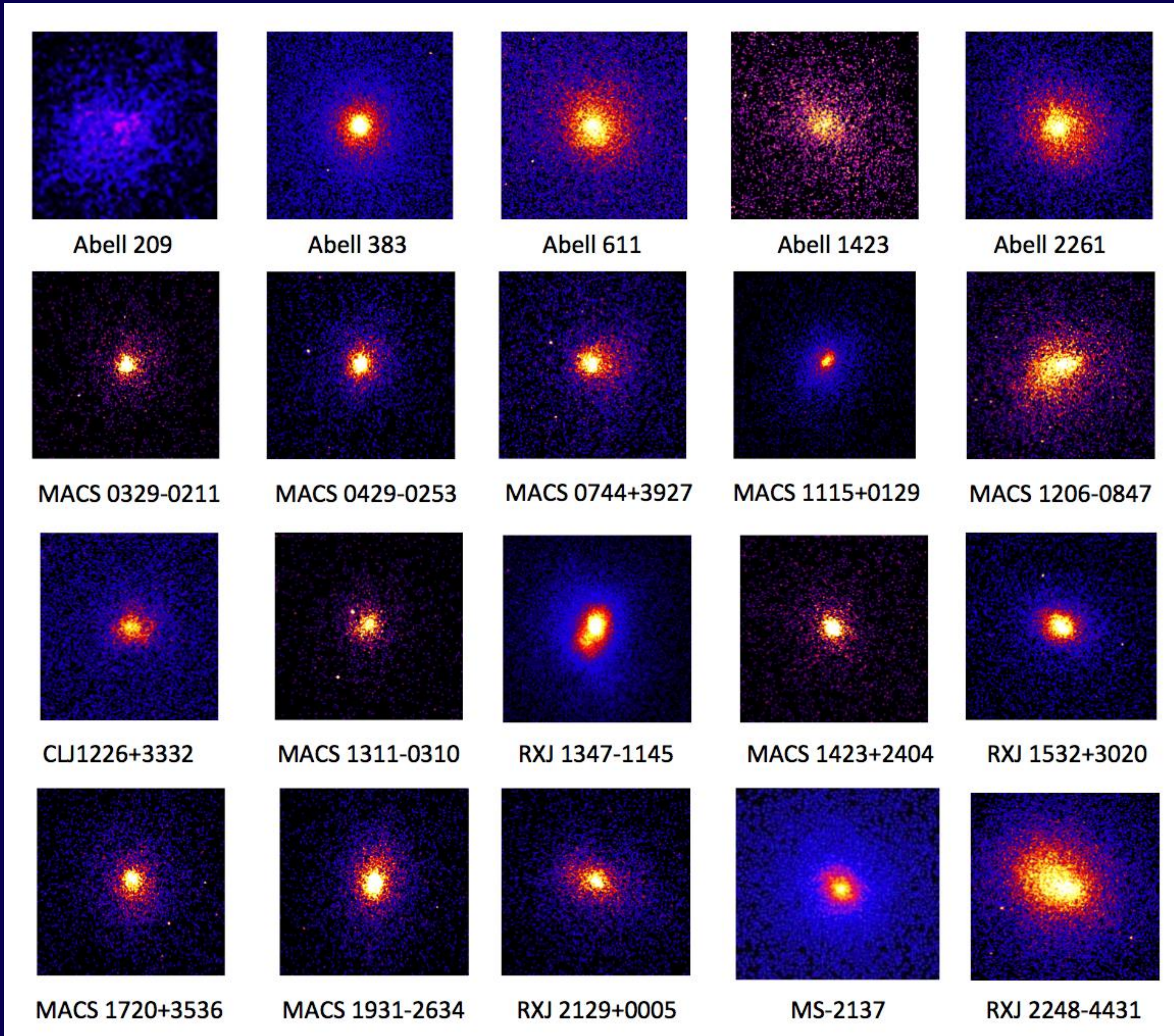

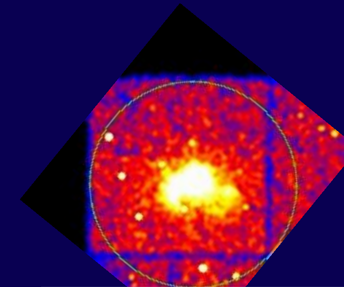

MACS 0717+3745

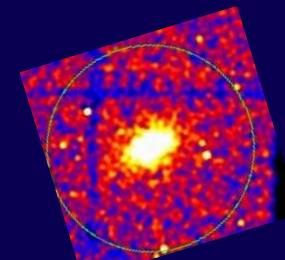

RXJ 0647+7015

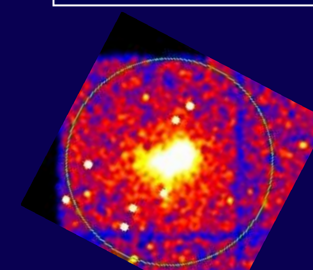

MACS 1149+2223

All have T_x > 5 keV

X-ray images of 23 of the 25 CLASH clusters. 20 are selected to be “relaxed” clusters (based on their x-ray properties only). 5 are selected specifically because they are strongly lensing **θ_E > 30”**

CLASH Characterization

Theoretical predictions from 1,400 clusters re-simulated at high spatial and mass resolution by Meneghetti+CLASH 14 (MUSIC-2: DM + adiabatic gas)

- CLASH X-ray selection function taken into account using Chandra X-ray image simulator (X-MAS).
- (M_{200}, c_{200}) measured both in 3D and 2D, taking into account projection effects → modest orientation bias for CLASH.
- The CLASH selection function gives a heterogeneous sample of relaxed (70%) and unrelaxed (30%) clusters.
- c200 recovered from the lensing analysis of the CLASH clusters are c=[3-6], with an average value of 3.9 and a standard deviation of 0.6.

Objective (1)

- Non-parametric mass profile reconstruction from joint shear-and-magnification analysis of 20 CLASH clusters
- Cluster mass measurements

20 CLASH clusters in Umetsu+14

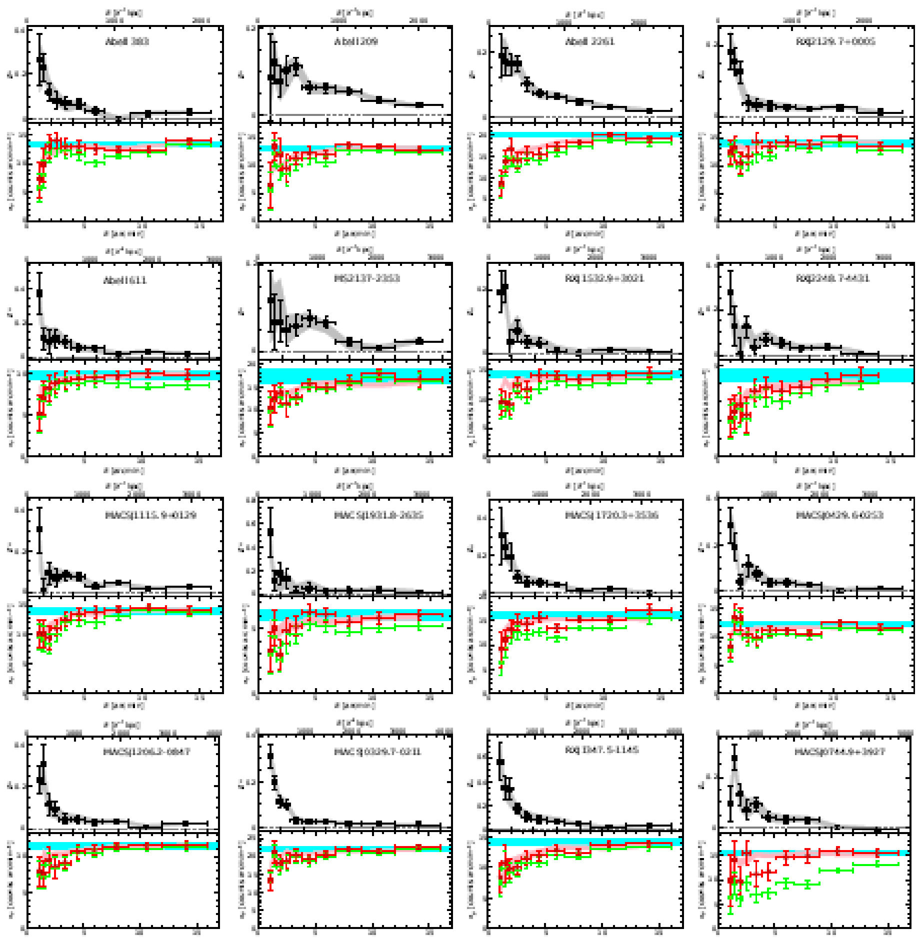

16 X-ray-selected clusters

- 15 clusters from 8.3m Subaru Telescope
- 1 southernmost cluster (RXJ2248) from 2.2m ESO/MPG
- $0.18 < z < 0.69$

$\langle\chi^2/\mathrm{dof}\rangle$ = 0.92 for 20 CLASH clusters

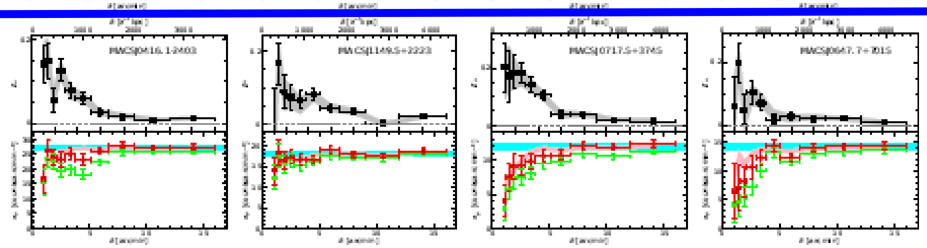

4 high-magnification clusters

- All 4 clusters from 8.3m Subaru Telescope

Joint Shear+Magnification Analysis

CLASH low mass

M_{vir}=6e14Msun/h (z=0.19)

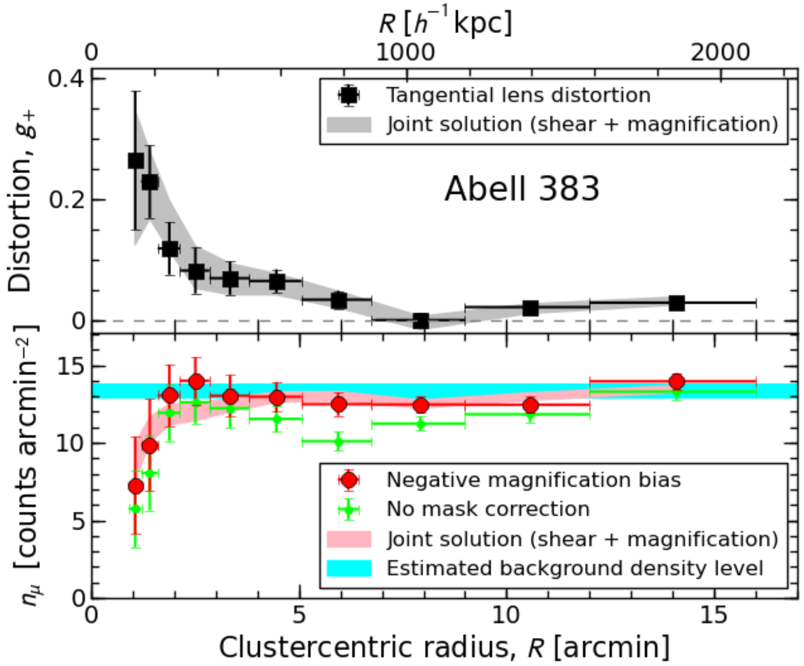

CLASH high mass

M_{vir}=23e14Msun/h (z=0.45)

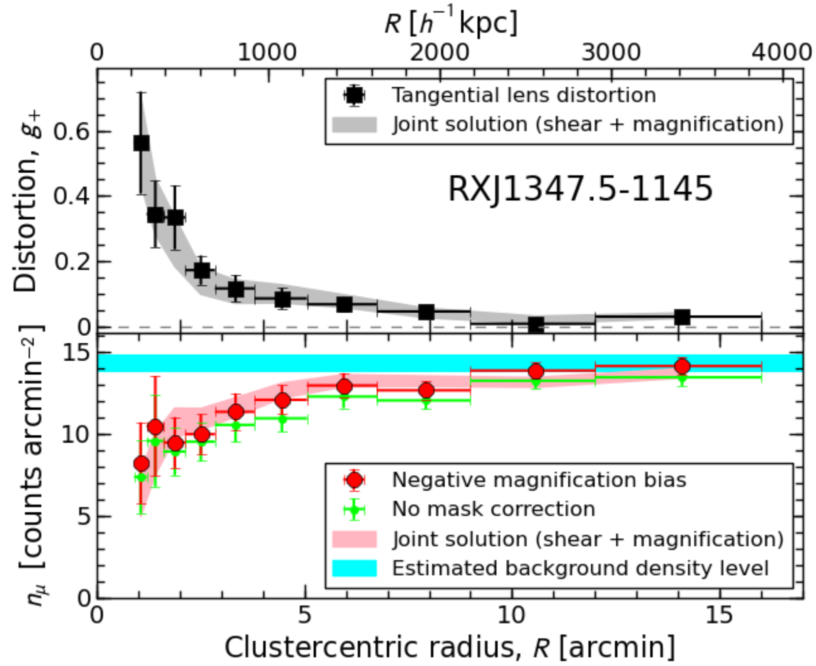

For all clusters, 2N=20 measurements, N+1=11 binned $\Sigma(R)$ parameters

Umetsu+CLASH 14, arXiv:1404.1375

Mass Density Profile Dataset

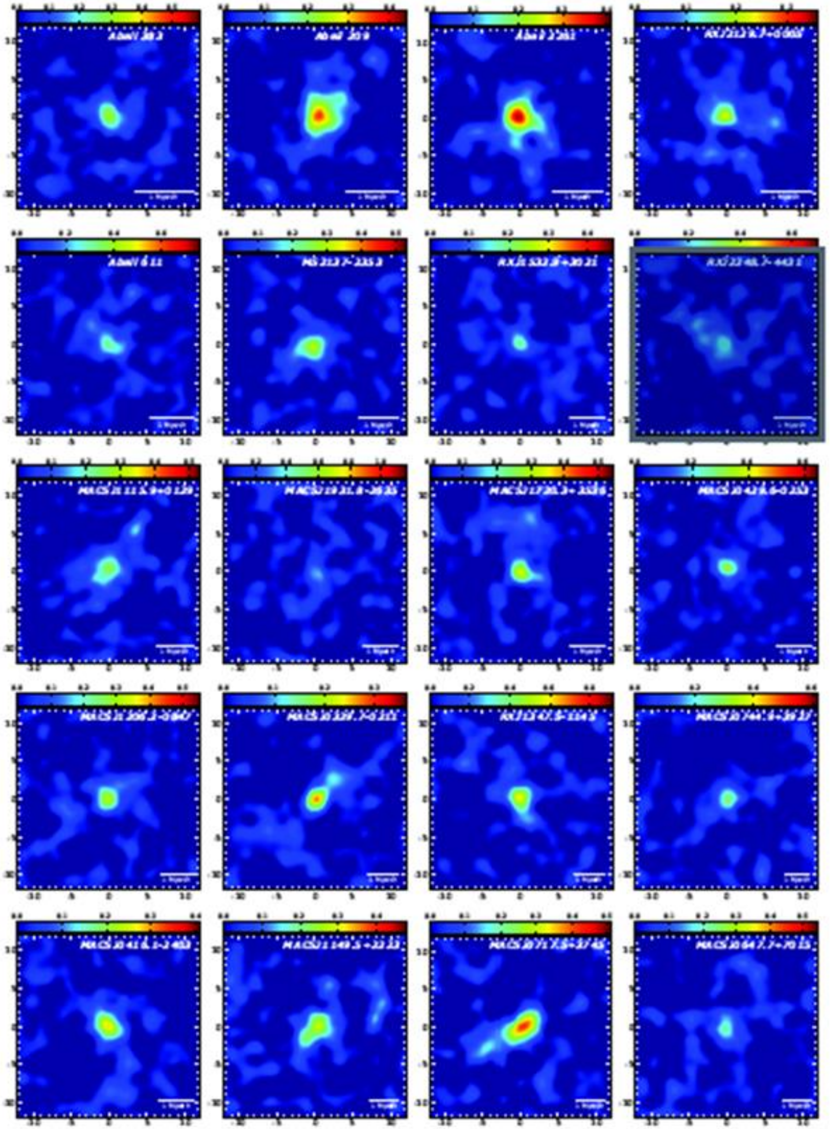

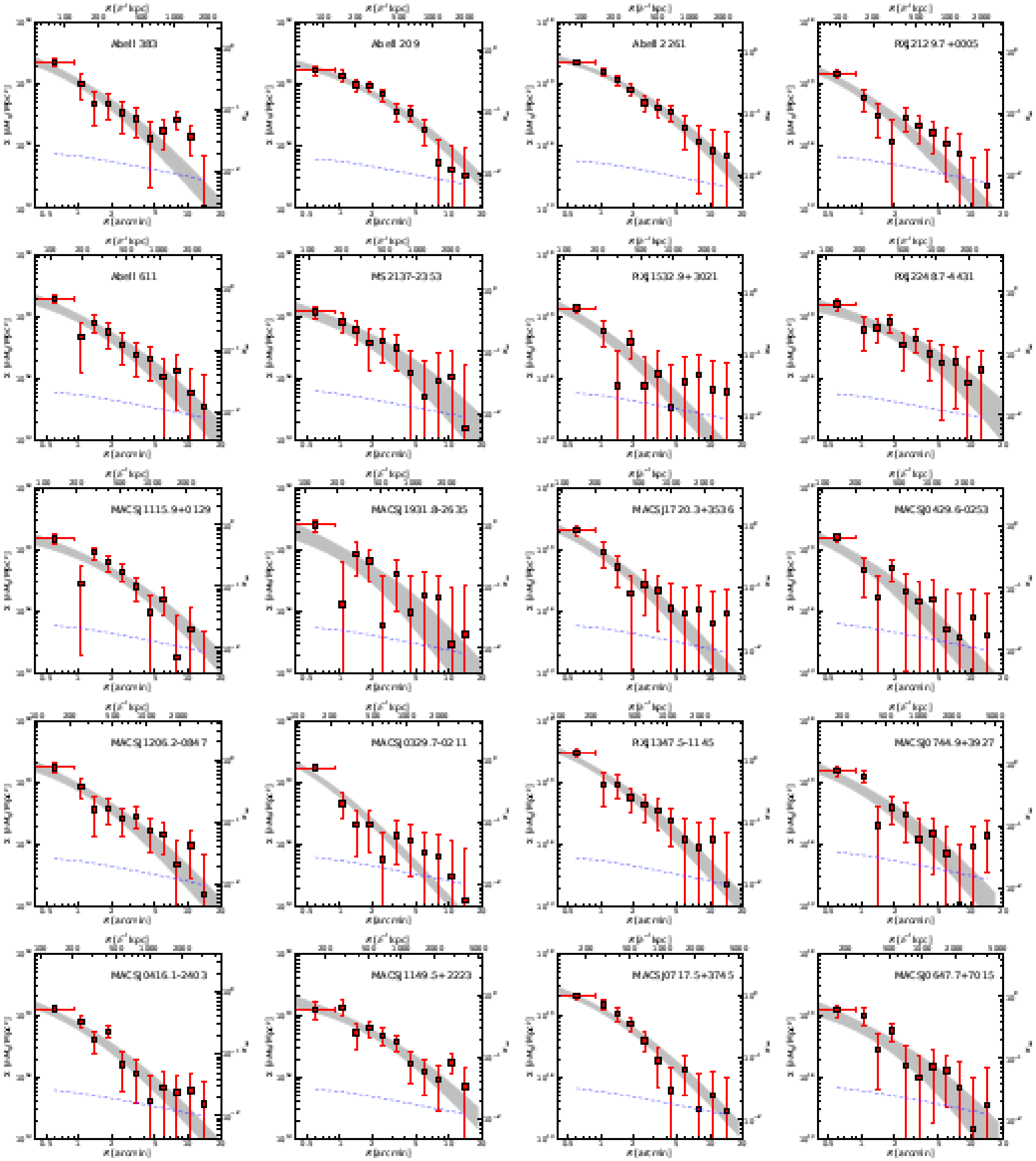

Shear-Magnification Consistency

Spherical NFW $M_{3D}(r)$ profiles for 20 CLASH clusters

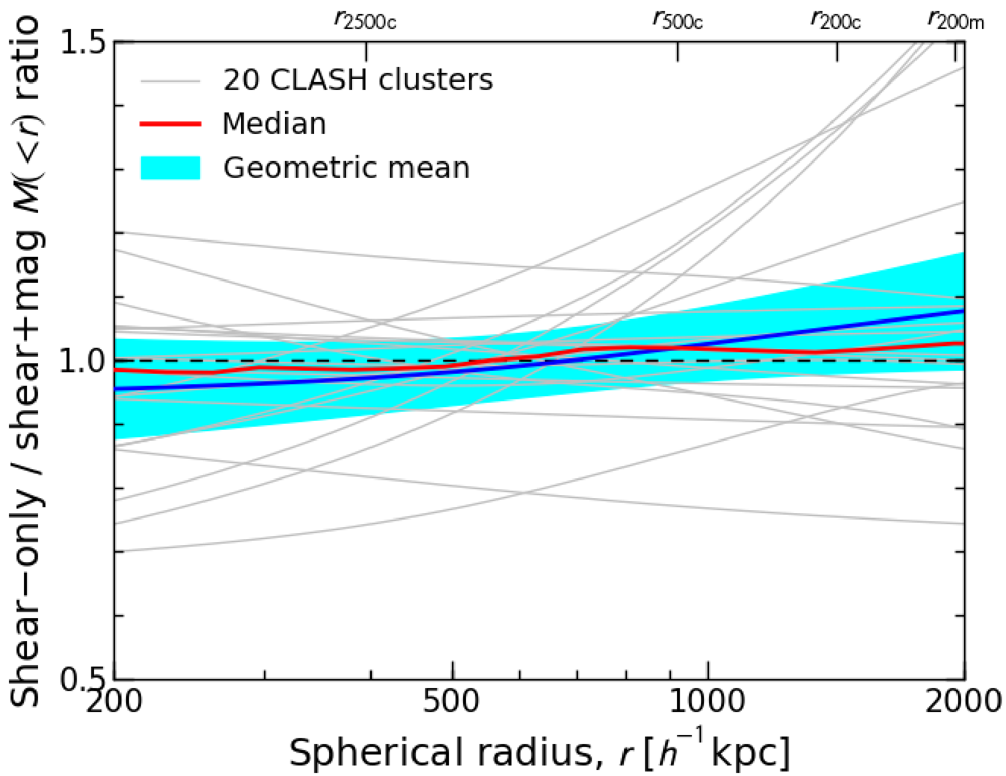

Systematic uncertainty in the overall mass calibration of about +/- 8 percent

Mass Comparisons @ R=1.5Mpc

Merten+CLASH 14

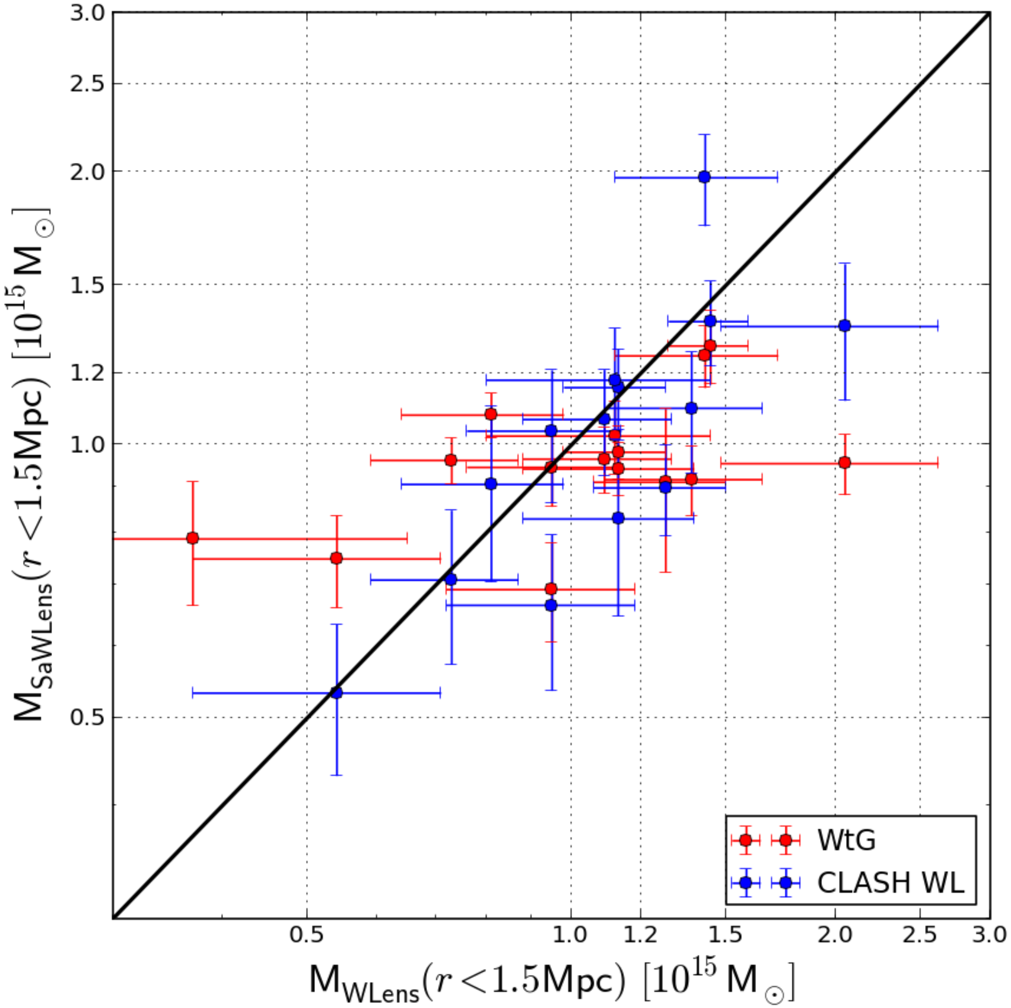

Un-weighted geometric mean mass ratios (<Y/X>=1/<X/Y>)

- <SaWLenS / WL> = 0.96
- <WL / WtG> = 0.91
- <SaWLenS / WtG> = 0.88

WL (Umetsu+14)
→ shear+mag (Subaru)
SaWLenS (Merten+14)
→ SL + shear (HST+Subaru)
WtG (Applegate+14)
→ shear (Subaru)

Note: WL mass calibration uncertainty of 8 percent

(contd.)

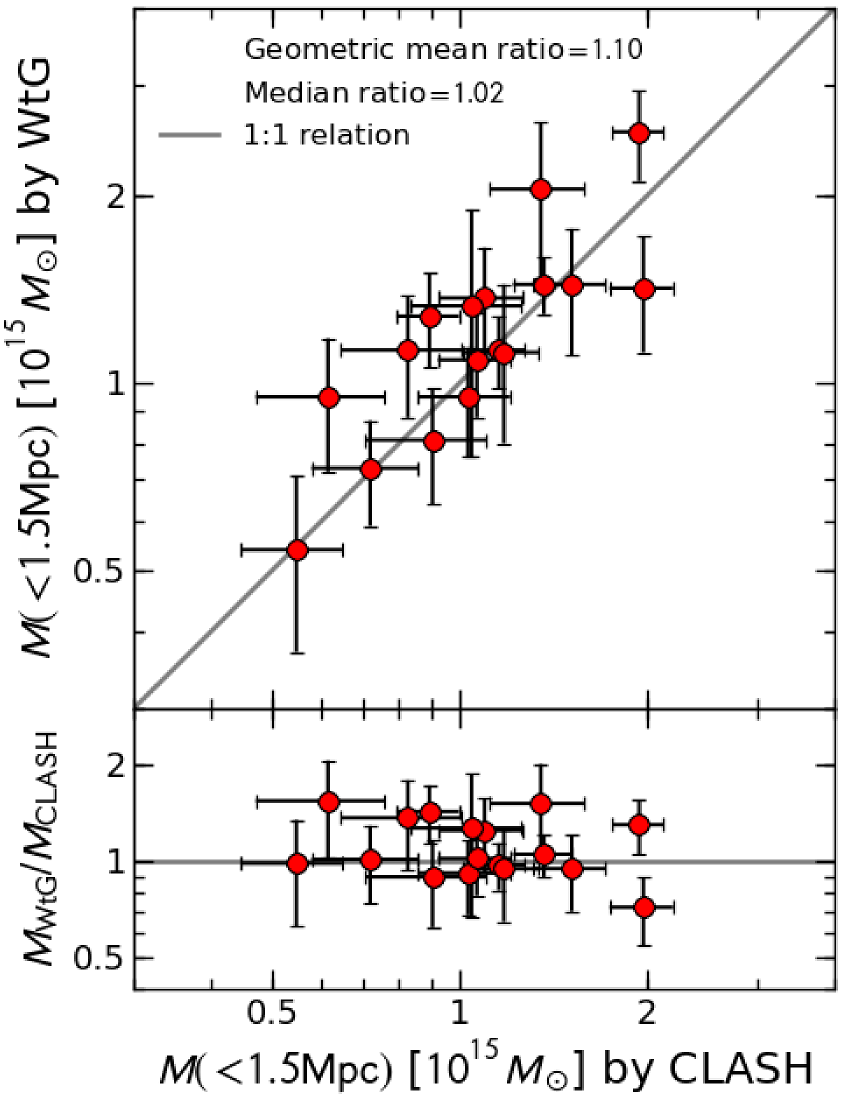

No obvious mass dependence

Umetsu+CLASH 14, arXiv:1404.1375

Comparisons with X-ray masses

Chandra HSE / CLASH-WL

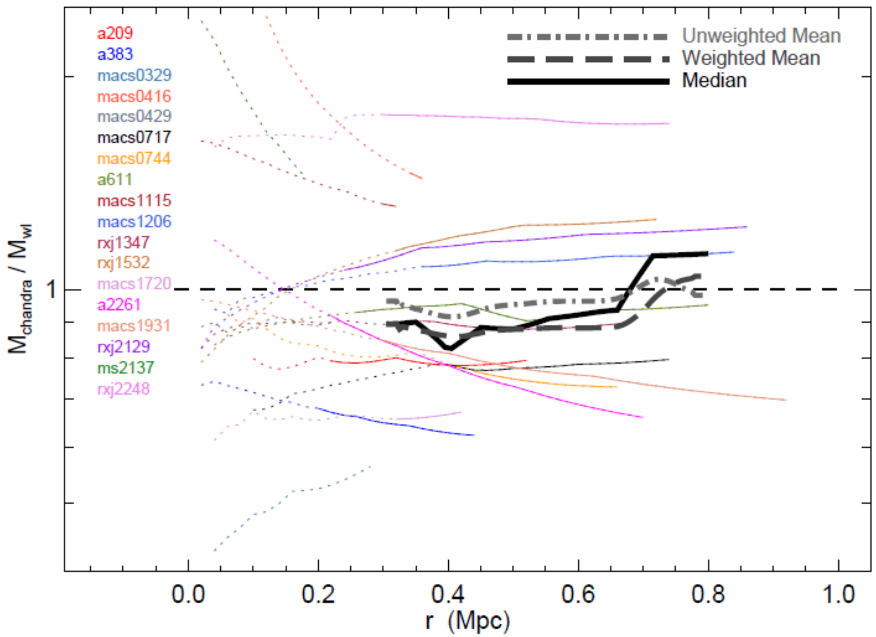

XMM HSE / CLASH-WL

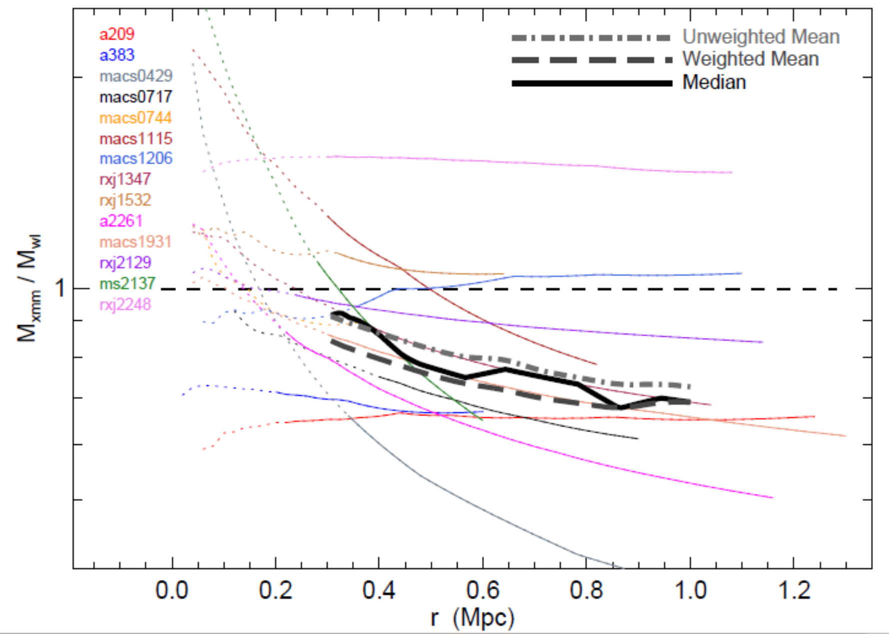

M_{chan}/M_{wl} = 0.95 +/- 0.07 +/- 0.08 @0.5Mpc

M_{xmm}/M_{wl} = 0.83 +/- 0.05 +/- 0.08 @0.5Mpc

M_{xmm}/M_{wl} = 0.73 +/- 0.10 +/- 0.08 @1.0Mpc

Donahue+CLASH 14, in prep

Objective (2)

- Ensemble-averaged halo mass profile $\Delta\Sigma(R)$
- Ensemble-averaged halo concentration

from stacked ***shear-only*** analysis of the CLASH X-ray-selected sample (16 clusters)

Ensemble-averaged DM halo (1h) density profile

Stacking of weak-lensing signals by weighting individual clusters according to the sensitivity kernel matrix:

$$\langle\langle \widehat{\Delta\Sigma_+} \rangle\rangle = \left(\sum_n \mathcal{W}_{+n}\right)^{-1} \left(\sum_n \mathcal{W}_{+n} \widehat{\Delta\Sigma}_{+n}\right),$$

with the individual sensitivity matrix

$$(\mathcal{W}_{+n})_{ij} \equiv \Sigma_{c,n}^{-2} \left(C_{+n}^{-1}\right)_{ij}$$

defined with the total covariance matrix

$$\mathcal{C}_+ = \mathcal{C}_+^{\mathrm{stat}} + \mathcal{C}_+^{\mathrm{sys}} + \mathcal{C}_+^{\mathrm{lss}}.$$

With "trace-approximation", averaging is interpreted as

$$\langle\langle \Sigma_c^{-1} \rangle\rangle = \frac{\sum_n \mathrm{tr}(\mathcal{W}_{+n})\Sigma_{c,n}^{-1}}{\sum_n \mathrm{tr}(\mathcal{W}_{+n})},$$

Umetsu+CLASH 14, arXiv:1404.1375

Stacked halo profile shape

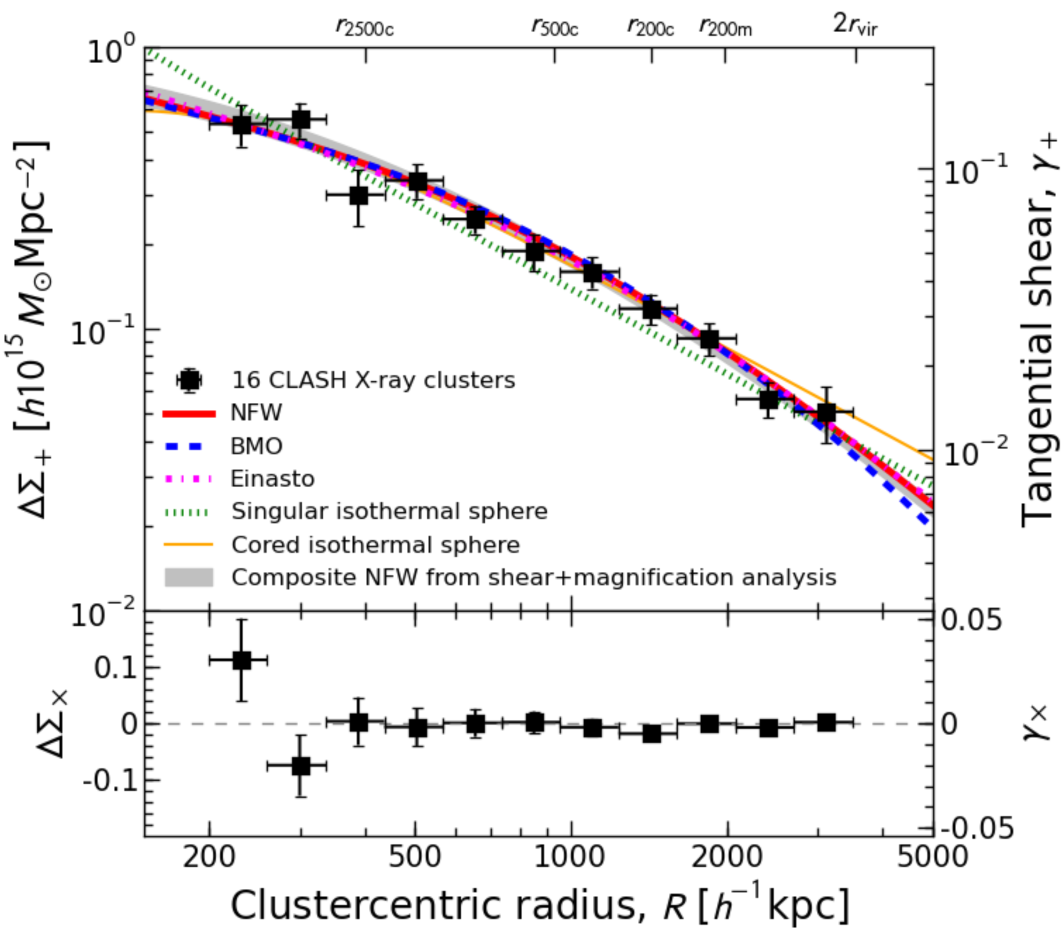

2-halo contribution (ν~3.8, b_h~9) is estimated to be γ_+ < 1e-3 within $2R_{vir}$

Stacked shear-only analysis provides a net 1-halo-only constraint.

Einasto shape parameter α=0.19 +/- 0.07, consistent with the NFW equivalent value of α~0.18

Consistent with a family of density profiles for collisionless, cold DM halos (NFW, variants of NFW, Einasto) Umetsu+CLASH14

Integrated constraints on c(M,z)

Theoretical predictions for stacked c-M-z

$$<<c>> = \frac{\int dM \int dz\, N(M,z)\,\hat{c}(M,z)}{\int dM \int dz\, N(M,z)} \approx \frac{\sum_n \mathrm{tr}(W_n)\,\hat{c}(M_n, z_n)}{\sum_n \mathrm{tr}(W_n)}$$

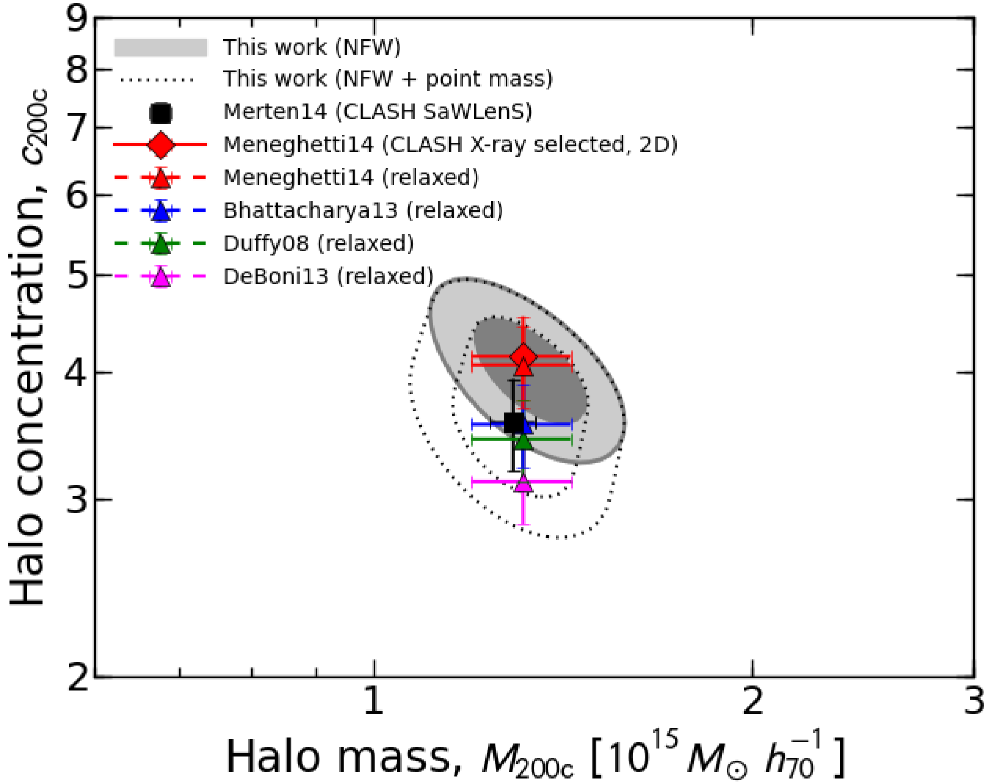

Variance in theory due to different cosmology and spatial resolution

M14: σ8=0.82

Bhat13: σ8=0.8

Duffy08: σ8=0.8

DeBoni13: σ8=0.78

Integrated constraints on c(M,z)

Theoretical predictions for stacked c-M-z

$$\langle\langle c \rangle\rangle = \frac{\int dM \int dz\, N(M,z)\,\hat{c}(M,z)}{\int dM \int dz\, N(M,z)} \approx \frac{\sum_n \mathrm{tr}(W_n)\,\hat{c}(M_n, z_n)}{\sum_n \mathrm{tr}(W_n)}$$

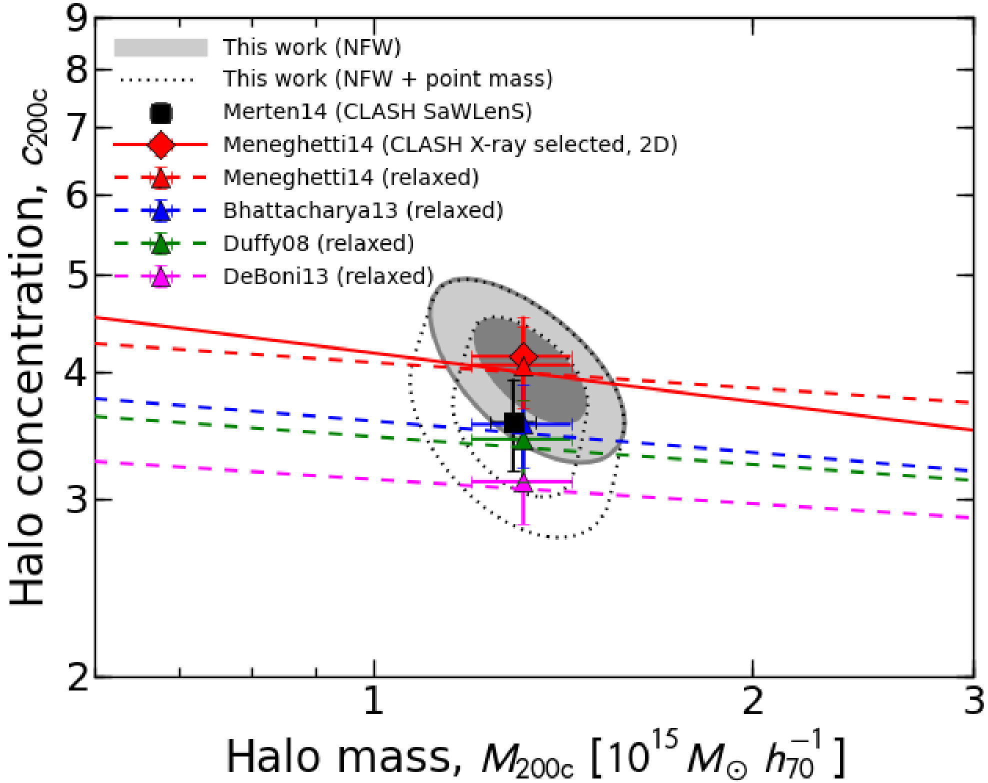

c-M curves

$$c = \hat{c}(M, \langle\langle z \rangle\rangle)$$

$$\langle\langle z \rangle\rangle = 0.35$$

Objective (3)

- Ensemble-averaged total mass profile
  $\Sigma(R)=\Sigma_{1h}(R)+\Sigma_{2h}(R)$

of individual total mass profiles of the CLASH X-ray-selected sample (16 clusters) reconstructed from joint shear+magnification analysis

Averaged cluster (1h) + LSS (2h) from combined shear + magnification

CLASH-WL: shear+magnification

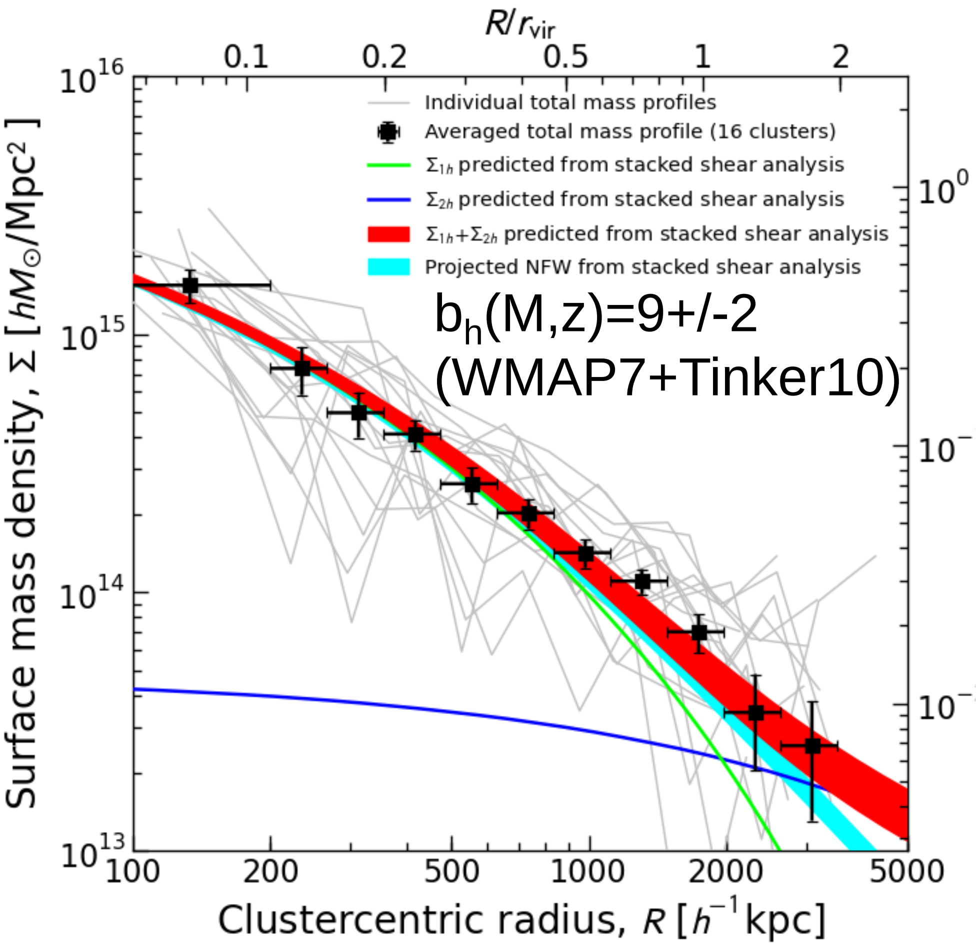

2D halo-model decomposition:

truncated NFW (BMO) + LCDM 2h term (Oguri & Hamana 11)

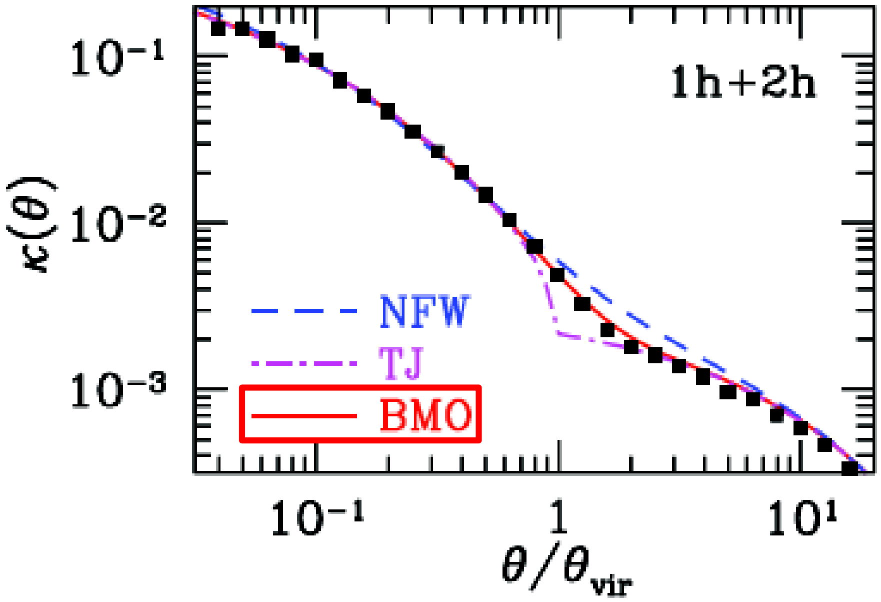

Umetsu+CLASH14

Comparison with pre-CLASH results

- **C200 vs θ_E relation, consistent with triaxial CDM halos (Oguri+12)**
- **Similar ν (MAH), similar Σ in outskirts (Diemer & Kravtsov 14)**
- **Increased c at R<0.5Mpc/h, consistent w orientation bias (Gao+12)**

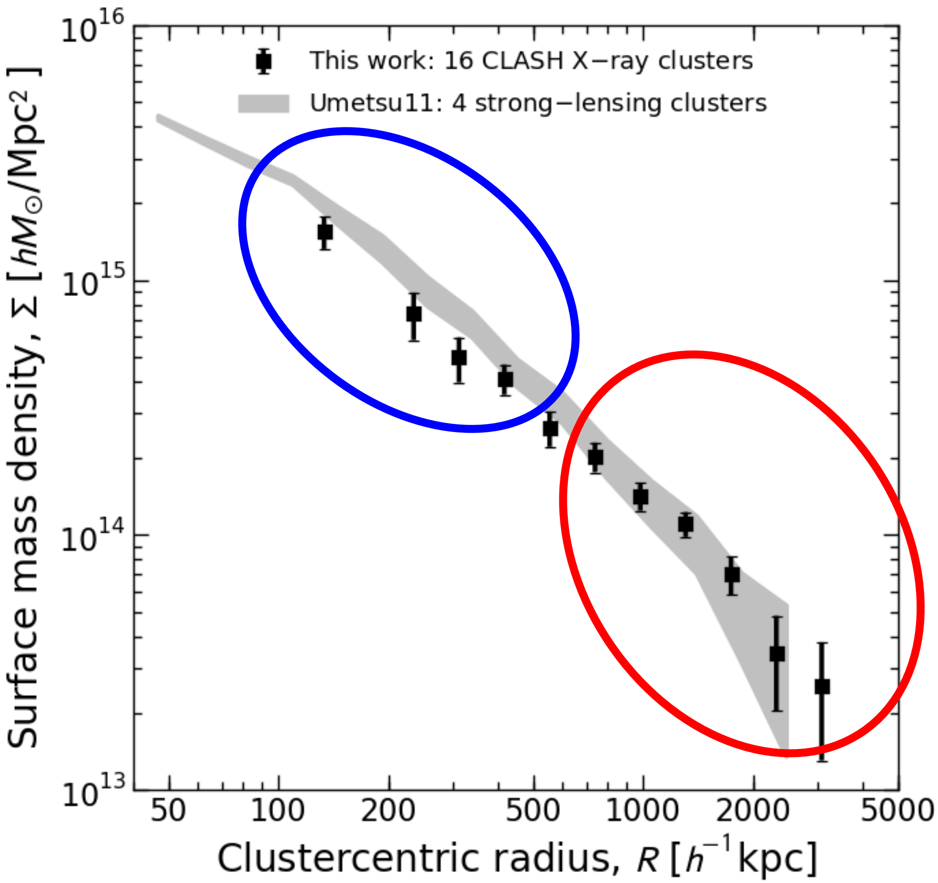

CLASH X-ray-selected sample

- M200 = 0.9e15Msun/h
- c200 = 4.0
- θ_E ~ 15” (zs=2)
- ν=3.8 (b~9)

Umetsu11b sample

- M200 = 1.2e15Msun/h
- c200 = 6.1
- θ_E ~ 36” (zs=2)
- ν=4.1 (b~11)

Umetsu+CLASH14

Summary

- Ensemble-averaged halo structure $\Delta\Sigma$ (1h) of X-ray-regular CLASH clusters is consistent with a family of standard (collisionless) DM predictions:
  - Halo mass: M_{200}= 1.3 +/- 0.1 $10^{15}M_{sun}$ at z=0.35
  - Einasto (PTE=0.51): degree of curvature, α=0.19 +/- 0.07
  - NFW (PTE=0.66): degree of concentration, c_{200}=4.01 (+0.35, -0.32)
- The measured concentration is in excellent agreement with the theoretical expectation, c_{200}= 4.15 +/- 0.40, which takes into account the CLASH selection function and projection effects (Meneghetti+CLASH 14).
- Our c-M results are consistent with the SaWLenS analysis of Merten+CLASH 14, demonstrating consistency between results obtained with different lensing methods.

Summary (contd.)

- Cluster masses from CLASH-WL, CLASH-SaW, WtG-WL are in agreement within the uncertainties: WtG-WL > CLASH-WL > CLASH-SaWLenS
  - <CLASH-WL / WtG> = 0.91
  - <SaWLenS / WtG> = 0.88
  - <SaWLenS / CLASH-WL> = 0.96
- Total matter distribution Σ (1h+2h) around clusters determined from shear+magnification is consistent with the shear-based halo model predictions, establishing further consistency in the context of LCDM.
  - Large modeling uncertainties in the 1h-2h transition region (Oguri & Hamana 11; Diemer & Kravtsov 14)
- Most of the previous overconcentration problems can be explained by
  - Theoretical predictions were likely underestimated (10-20%) in the high-mass cluster regime, M200>5e14Msun/h (σ8, resolution, ..)
  - Orientation bias due to halo triaxiality, boosting Σ(R) at R<500kpc/h (Gao+12), resulting in ~+50% bias in c200 (Hennawi+07; Oguri+12)

Supplemental Slides

Scatter in $M_{2D}(R)$ by halo triaxiality

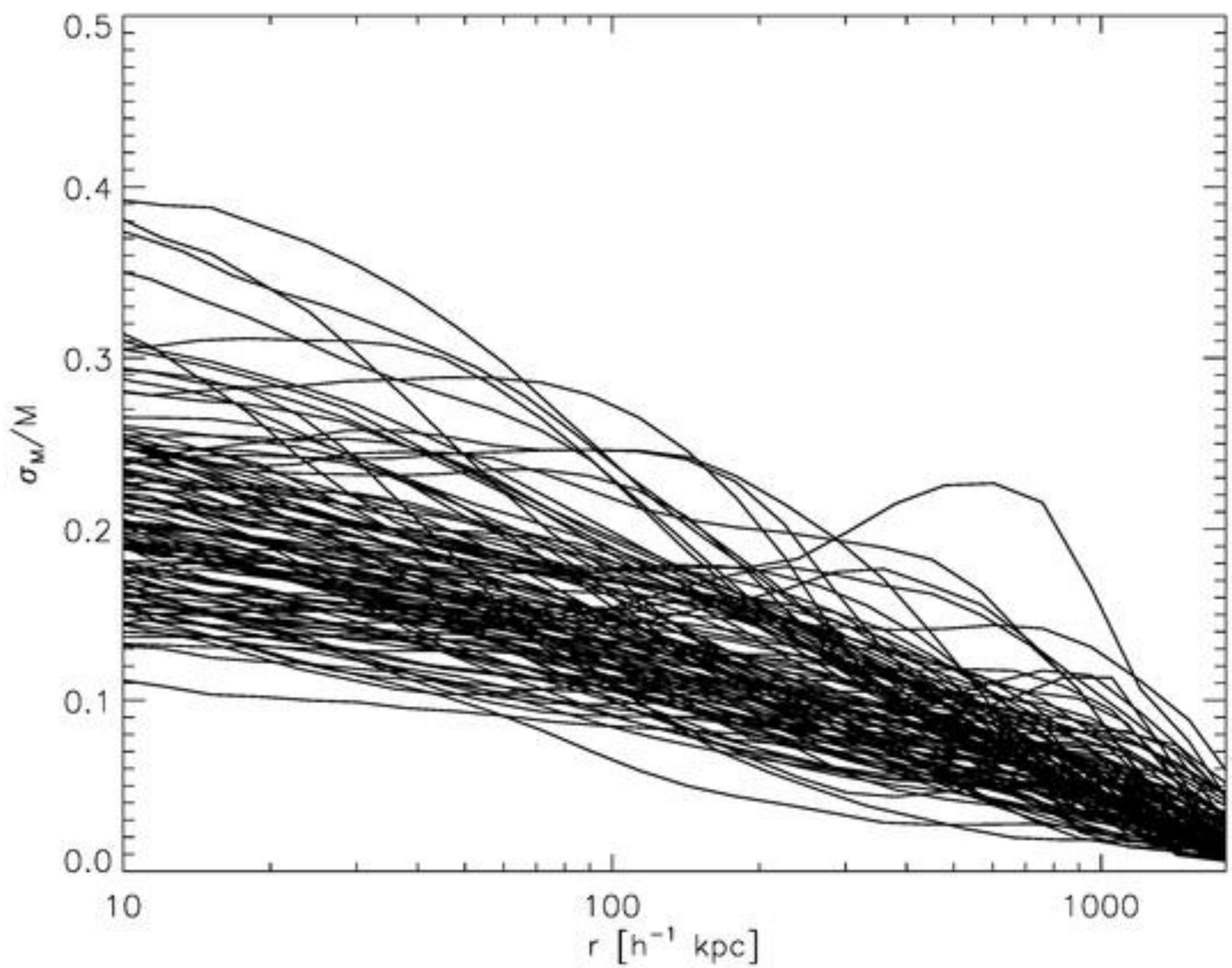

MUSIC-2 simulation by Massimo

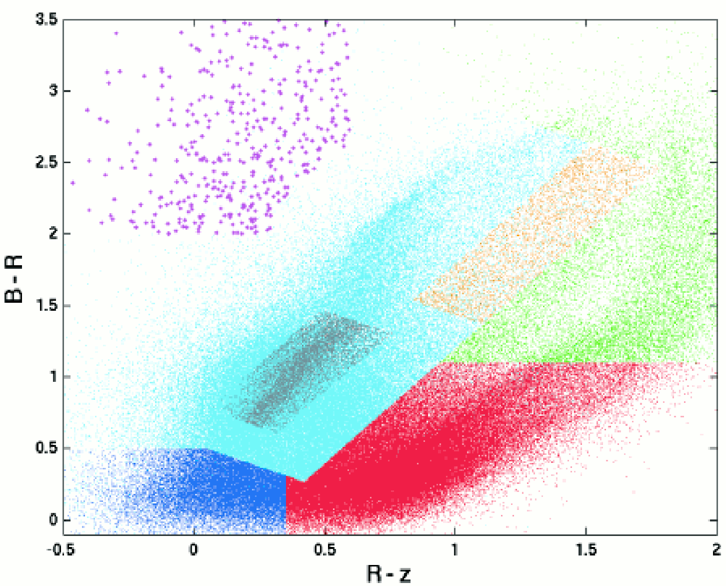
B - R
R - z
3.5
3
2.5
2
1.5
1
0.5
0
-0.5
0
0.5
1
1.5
2

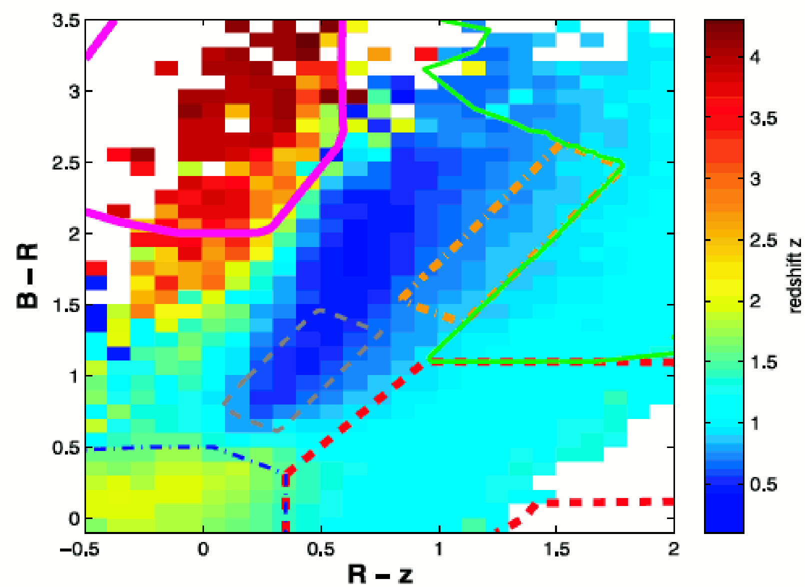
B – R
R – z
redshift z
3.5
3
2.5
2
1.5
1
0.5
0
–0.5
0
0.5
1
1.5
2
4
3.5
3
2.5
2
1.5
1
0.5

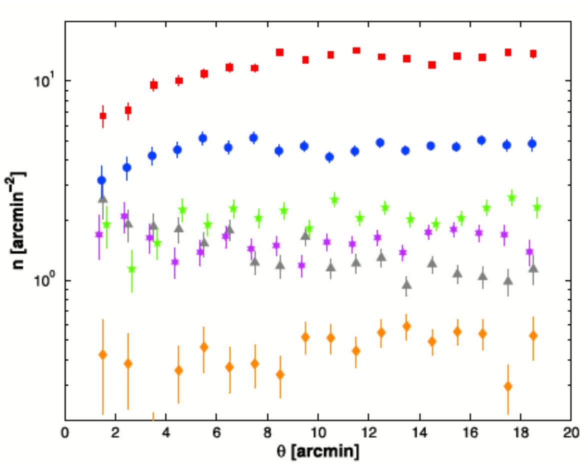
n [arcmin^{-2}]
θ [arcmin]
10^1
10^0
0
2
4
6
8
10
12
14
16
18
20

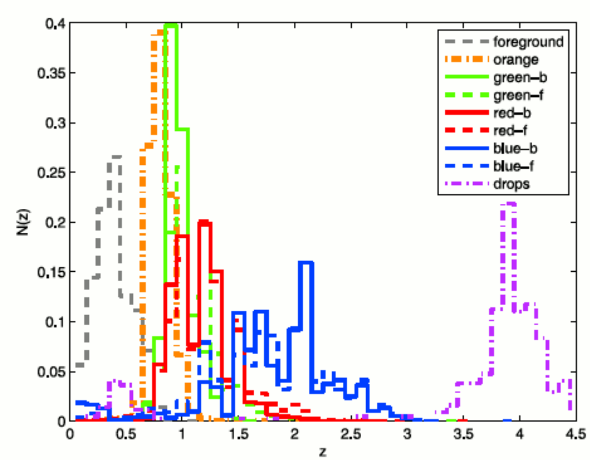
N(z)
z
foreground
orange
green–b
green–f
red–b
red–f
blue–b
blue–f
drops
0.4
0.35
0.3
0.25
0.2
0.15
0.1
0.05
0
0
0.5
1
1.5
2
2.5
3
3.5
4
4.5

Cluster masses recovered from lensing analysis

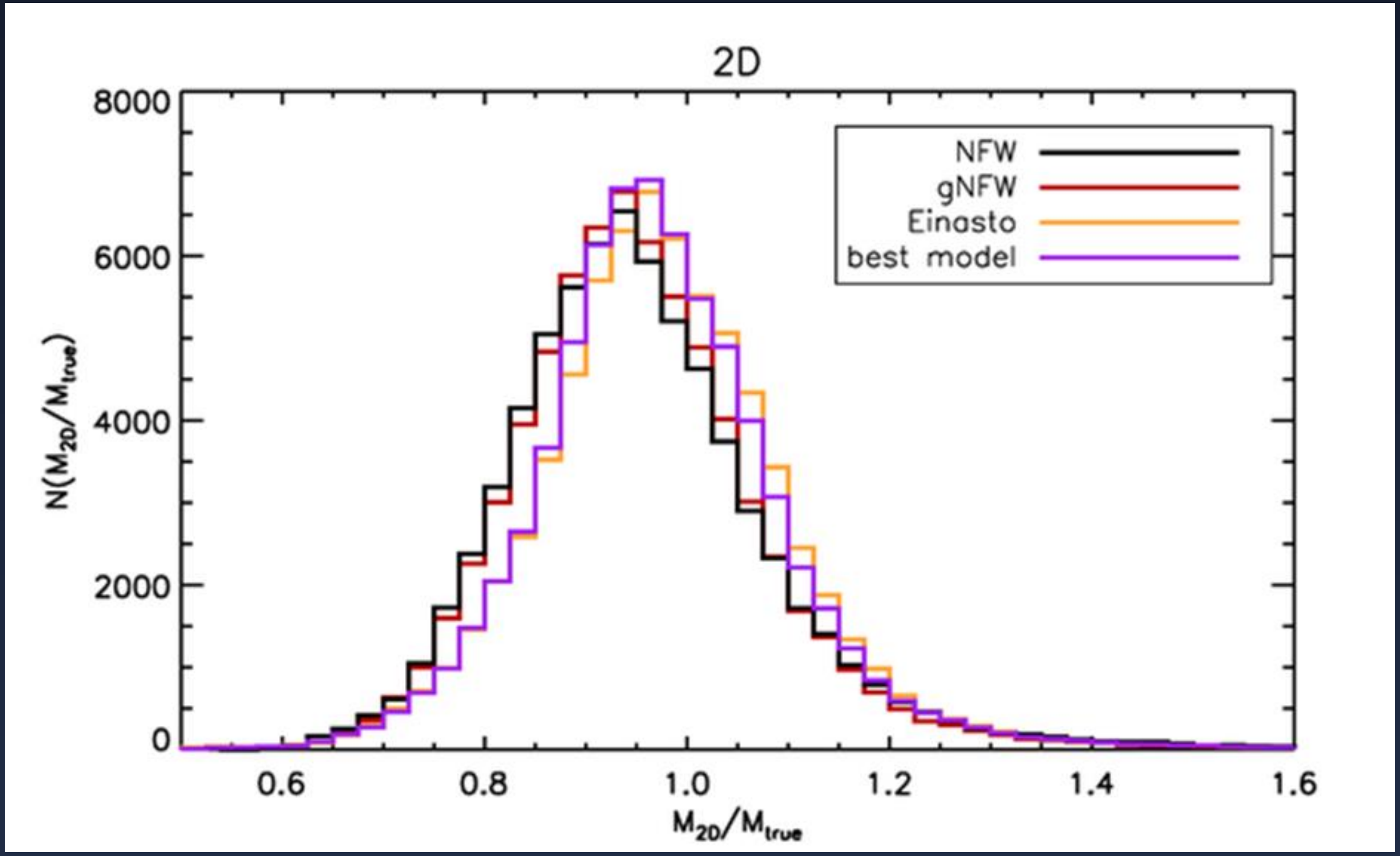

Meneghetti+CLASH 14

Magnification bias effects

Flux-limited source counts:

$$n_{\mathrm{obs}}(>f) = \mu^{-1} n(>\mu^{-1} f)$$

Broadhurst, Taylor & Peacock 95

Geometric area distortion

n/μ

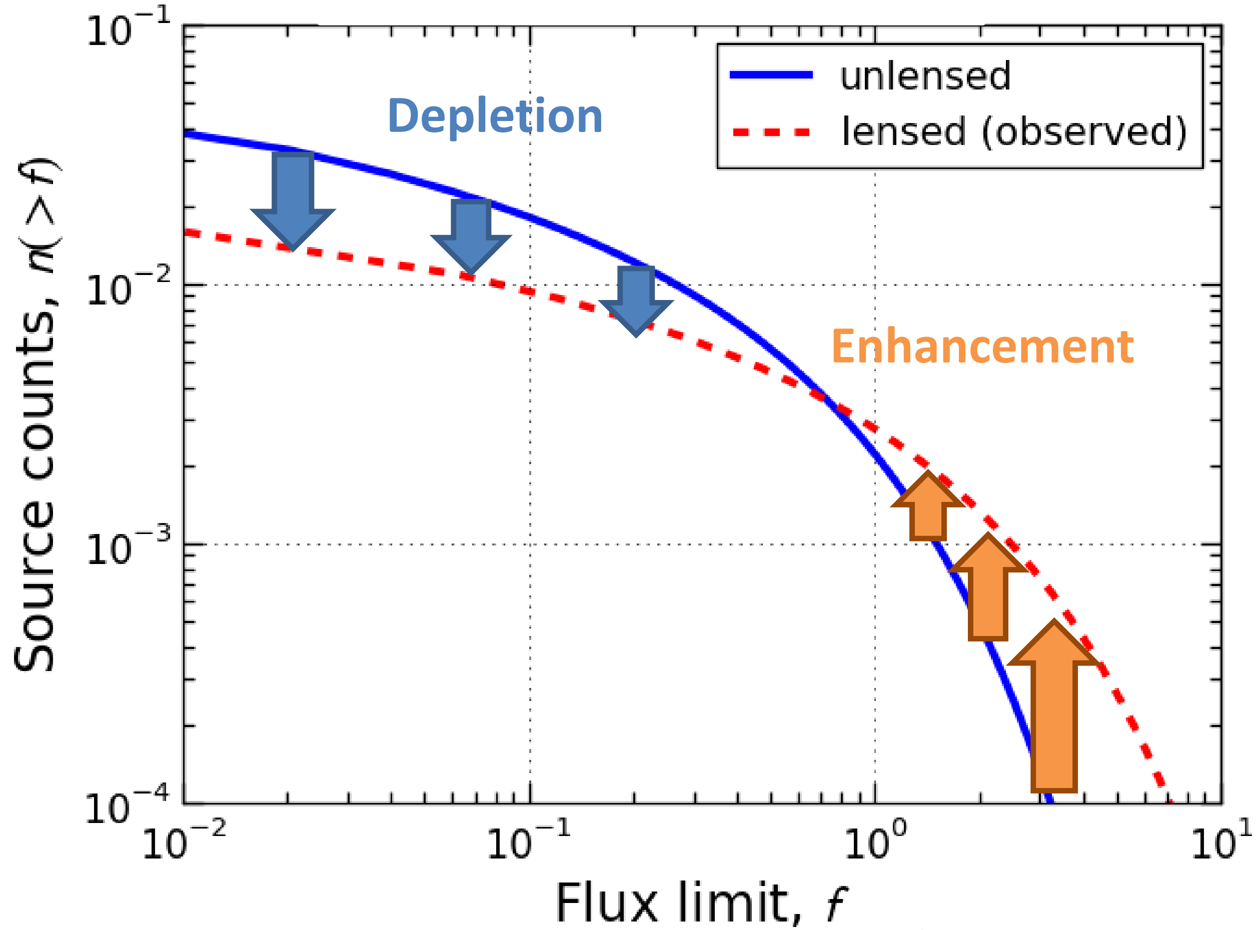

Flux amplification